Unified analytical algorithmic framework for diverse terrain effects on various external gravity field elements

PAGravf4.5; https://www.zcyphygeodesy.com/en/
ZHANG Chuanyin; zpmzsyzcy1968@163.com
Chinese Academy of Surveying & Mapping
March 2026, Beijing, 100830, China

7.4 Classical Terrestrial Gravity Reduction Schemes and Their Limitations

The classical Stokes boundary value problem defines the geoid as the boundary surface, with both the Bouguer gravity anomaly and isostatic gravity anomaly are strictly defined on this equipotential surface. Traditional gravity reduction essentially involves the analytic downward continuation of gravity observables from the Earth's surface (or near-Earth space) to the geoid, incorporating corrections for topographic mass effects.

7.4.1 Free-Air Correction and Gravity Anomaly

The gravity g on the geoid can be expressed in terms of terrestrial gravity g_s via a Taylor series expansion:

$$g = g_s - \left(\frac{\partial g}{\partial h}\right)_N h - \frac{1}{2}\left(\frac{\partial^2 g}{\partial h^2}\right)_N h^2 - \cdots = g_s + \Delta_1 g \tag{4.1}$$

where $\Delta_1 g$ denotes the Free-Air Correction. This term represents the increment required to analytically continue g_s downward to the geoid when neglecting the topographic masses between the surface and the geoid.

Since the actual vertical gravity gradient on the geoid is unknown, it is conventionally approximated by the normal gravity gradient, truncating higher-order terms (typically retaining up to the second order):

$$\Delta_1 g = -\left(\frac{\partial \gamma}{\partial h}\right)_N h - \frac{1}{2}\left(\frac{\partial^2 \gamma}{\partial h^2}\right)_N h^2 \tag{4.2}$$

Using approximations for the normal gradient, $\Delta_1 g = 0.3086h - 1.5 \times 10^{-7}h^2 \approx 0.3086h$ mGal, where h is the orthometric (or normal) height in meters.

Consequently, the gravity anomaly on the geoid is formulated as:

$$\Delta g = g - \gamma_0 = g_s - \gamma_0 + \Delta_1 g \tag{4.3}$$

where g is the gravity on the geoid, and γ_0 is the normal gravity on the normal ellipsoid.

Comparing the terrestrial gravity anomaly $(\Delta g_s = g_s - \gamma_\zeta)$ with the geoid-defined gravity anomaly $(\Delta g = g - \gamma_0)$, a more rigorous approach than the simplified free-air correction mentioned above is to directly perform analytic continuation on the gravity anomaly field itself, utilizing the functional relationship between Δg_s and Δg.

7.4.2 Bouguer Plate Correction and Local Terrain Correction

Assuming planar geometry for both the Earth's surface (terrain surface) and the geoid, the gravitational attraction of the topographic mass (modeled as an infinite planar slab of thickness h at point P) is $2\pi G\rho h$. Removing this mass yields the Bouguer Plate Correction

(or Simple Bouguer Correction):

$$\Delta_2 g = -2\pi G\rho h \tag{4.4}$$

where G is the gravitational constant. With a standard topographic density $\rho = 2.67 \times 10^3$kg/m^3, this simplifies to $\Delta_2 g = -0.1118h$ mGal.

Also known as the Planar Layer Correction, this induces a geopotential change $\Delta_2 V = 2\pi G\rho h S/R$, where S is the base area of the planar layer, and R is the average radius of the Earth. Since $\lim_{S\to\infty} \Delta(\Delta_2 V) \neq 0$, the resulting geopotential is non-harmonic. Thus, the planar Bouguer correction fundamentally violates the harmonic property of the Earth's external gravitational field.

The planar assumption implies a flat surrounding terrain. To account for real topographic relief, one must subsequently remove masses above the computation point and fill voids below it in the vicinity.

This residual term is the Local Terrain Correction ($\Delta_3 g$). Unlike the Bouguer plate correction, both the Free-Air correction ($\Delta_1 g$) and Local Terrain correction ($\Delta_3 g$) are analytic operations that preserve the harmonic nature of the field.

7.4.3 Bouguer Anomaly and Gridding Computation

The Bouguer Gravity Anomaly (or simply Bouguer Anomaly) defined on the geoid, is given by:

$$\Delta g_b = \Delta g + \Delta_2 g + \Delta_3 g = g_s - \gamma_0 + \Delta_1 g + \Delta_2 g + \Delta_3 g \tag{4.5}$$

The sum $\Delta_b g = \Delta_2 g + \Delta_3 g$ constitutes the Bouguer Correction. Due to the planar slab assumption, these are often termed "Simple" or "Planar" anomalies/corrections. Critically, the Bouguer correction alters the Earth's total mass distribution, thereby making the geoid and the external gravity field change.

The Bouguer gravity anomalies, defined on an equipotential surface with topographic masses effects removed, are generally believed to be smoother than the free-air gravity anomalies on the geoid. Consequently, gridding or prediction based on Bouguer gravity anomalies typically yields lower interpolation errors.

Grid averaging usually employs algorithms with translational invariance (isotropy). The mean Bouguer anomaly for a grid cell centered at (λ, φ) is expressed as:

$$\overline{\Delta g_b}(\lambda, \varphi) = \left[\sum_k f(\lambda_k - \lambda, \varphi_k - \varphi) \Delta g_b(\lambda_k, \varphi_k)\right] \tag{4.6}$$

where f is the two-dimensional kernel function. Common kernels include Inverse Distance Weighting, Shepard's Method, Multi-Quadric Interpolation, Kriging, and Radial Basis Functions.

Technical Note: If a gridding algorithm does not inherently satisfy the analytic functional relationships of the gravity field, operations should be performed on a gravity equipotential surface (e.g., the geoid) to minimize signal distortion. Direct gridding of terrestrial gravity anomalies on the non-equipotential terrain surface is theoretically inadvisable without prior rigorous harmonic reduction.

7.4.4 Limitations of Classical Gravity Reduction

Classical reduction schemes rely on the approximation $\Delta_1 g = -0.3086h + O(h^2)$ mGal,

which accounts solely for the normal gravity gradient. However, in regions with moderate relief (hundreds of meters), the contribution of the disturbing gravity gradient can reach or exceed the mGal level. A rigorous workflow should first compute normal gravity and gravity anomalies at observation points using exact formulas, followed by strict analytic continuation of the anomaly field to the geoid.

Furthermore, the classical concept of terrain correction is restricted to terrestrial gravity observations. The classical direct topographic effect specifically refers to the influence of topography on gravity (disturbance/anomaly), while the indirect topographic effect specifically refers to the influence of topography on the geopotential (disturbing potential/height anomaly/geoid undulation). Modern gravimetry encompasses diverse data types from space, airborne, marine, and terrestrial platforms, requiring a unified treatment of topographic effects on all gravity field elements (both on and outside the geoid).

Contemporary physical geodesy demands a comprehensive handling of these topographic effects across all gravity field elements. Traditional concepts like "Free-Air Correction", simple "Terrain Correction", and “Direct/Indirect Topographic Effect” are insufficient for high-precision applications.

PAGravf4.5 addresses these limitations by implementing a comprehensive algorithm framework capable of rigorous analytic treatment to diverse terrain effects on all gravity field elements on and outside the geoid.

7.5 Algorithms for Land-Sea Complete Bouguer Effects and Residual Terrain Effects

In physical geodesy, the treatment of topographic mass effects on various gravity field elements serves two fundamental objectives:

(a) Spectral Separation: To isolate ultra-short-wavelength components from discrete anomalous gravity field elements, thereby enhancing the performance of prediction, gridding, and numerical modeling.

(b) Approximation Enhancement: To improve the approximation of the ultra-short-wavelength gravity field by explicitly modeling the topographic mass contribution during gravity field recovery.

Crucially, for the second objective, maintaining the analytic functional relationships among topographic effects on various gravity field elements across different locations is a mandatory requirement of gravity field approximation theory.

Any anomalous gravity field element at an external point can be expressed as a linear combination of the disturbing potential (T), the gravity disturbance (δg), or their partial derivatives in the local coordinate system defined on the equipotential surface passing through the point. For instance, vertical deflections correspond to horizontal derivatives of T, while disturbing gravity gradients relate to vertical derivatives of δg. Consequently, solving the topographic mass effect problem for T and δg inherently provides the solution for all other gravity field elements.

7.5.1 Spherical Approximation Algorithm for Land Complete Bouguer Effects

The gravitational field generated by land topographic masses is termed the Land Complete Bouguer Effect. It represents the total effect of masses located between the terrain surface and the geoid on external gravity field elements.

The Unified Land-Sea Complete Bouguer Effect at any external point (See Figure 7.4 for the fundamental principle) is defined as the sum of:

- The effect of land topographic masses (between the surface and the geoid).
- The effect of seawater compensation masses (density change from ρ_w to ρ).

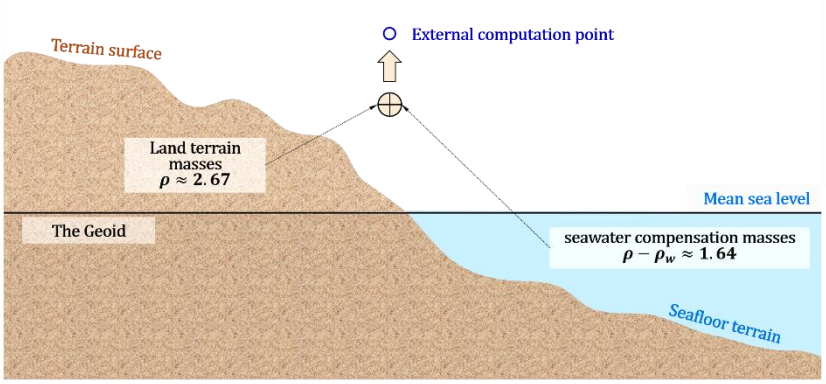

Figure 7.4: Fundamental Principle of Unified Land-Sea Complete Bouguer Effect

Neglecting atmospheric mass, the disturbing potential T at an external point is decomposed as:

$$T = T^{NT} + T^t = T^{NT} + T^B + T^R \tag{5.1}$$

where:

T^t: Gravitational potential of all topographic masses (Complete Bouguer Effect).

T^B: Potential of the spherical shell masses with thickness equal to the topographic elevation (Spherical Shell Bouguer Effect).

T^R : Potential of local topographic masses (Local Terrain Effect).

T^{NT} : Disturbing potential after removing topographic masses (Land Complete Bouguer Disturbing Potential).

Given that T is harmonic in external space, T^B, T^R, and T^t are likewise harmonic. Under the spherical approximation, the complete Bouguer effect on the disturbing potential in near-Earth space ($r \geq R + h$) can be expanded by h/R as:

$$T^t = T^B + T^R = 4\pi G\rho_0 \frac{R^2 h}{r}\left(1 + \frac{h}{R} + \frac{h^2}{3R^2}\right) + T^R \tag{5.2}$$

where: h is the terrain elevation directly beneath the external computation point, r is the geocentric distance of the computation point, and $\rho_0 = 2.67\times10^3 \mathrm{kg/m^3}$ is the mean topography density from the ground to the geoid.

Similarly, the gravity disturbance δg decomposes as:

$$\delta g = -\frac{\partial T^{NT}}{\partial r} - \frac{\partial T^t}{\partial r} = \delta g^{NT} + \delta g^t = \delta g^{NT} + \delta g^B + \delta g^R \tag{5.3}$$

where:

δg^t: Gravity (disturbance) of all topographic masses (Complete Bouguer Effect).

δg^B: Gravity (disturbance) of the spherical shell masses with thickness equal to the terrain elevation (Spherical Shell Bouguer Effect).

δg^R Gravity (disturbance) of local topographic masses (Local Terrain Effect).

δg^{NT}: Gravity disturbance removing topographic masses (Land Complete Bouguer gravity disturbance).

Under spherical approximation, the complete Bouguer effect on gravity disturbance is:

$$\delta g^t = \delta g^B + \delta g^R = 4\pi G\rho_0 \frac{R^2 h}{r^2}\left(1 + \frac{h}{R} + \frac{h^2}{3R^2}\right) + \delta g^R \tag{5.4}$$

Note: Eqs. (5.2) and (5.4) are truncated at the second order of h/R, making them suitable for terrestrial and airborne applications but insufficient for satellite altitudes.

7.5.2 Integral Algorithms for Local Terrain Effects in External Space

(1) Rigorous Integral Formulation

Assuming a constant terrain density = ρ_0 , the rigorous integral expression for the local terrain effect on the disturbing potential is:

$$T^R = \gamma\zeta^R = G\rho \iint_s \int_{R+h}^{R+h'} L^{-1}(r, \psi, r')\, dr'\, ds \tag{5.5}$$

where $ds = r'^2 cos\varphi' d\varphi' d\lambda'$ is the integration area element, r' is the geocentric distance of the integration area element (the moving point), and $L = \sqrt{r^2 + r'^2 - 2rr'cos\psi}$ is the Euclidean distance between the computation point and the volume element $dV = dr'ds$. The inner integral yields:

$$\int L^{-1}(r, \psi, r')\, dr' = ln(r' - rt + L) + C \tag{5.6}$$

where $t = cos\psi$ and C is the integration constant.

Singularity Handling: When the computation point coincides with the integration moving point, the integral becomes singular. The singular value is:

$$T^R|_0 = \frac{1}{6} G\rho A_0 \sqrt{A_0/\pi}\left(h_{xx} + h_{yy}\right) \tag{5.7}$$

where A_0 is the area of the integration area element at the computation point; h_{xx}, h_{yy} are the second-order horizontal partial derivatives of the terrain elevation at the computation point in the north (x) and east (y) directions, respectively.

The rigorous integral for the local terrain effect on gravity disturbance is:

$$\delta g^R = -T_r^R = -\frac{\partial T^R}{\partial r} = -G\rho \iint_s \int_{R+h}^{R+h'} \frac{\partial L^{-1}(r,\psi,r')}{\partial r} dr' ds \tag{5.8}$$

with the inner integral:

$$\int \frac{\partial L^{-1}(r,\psi,r')}{\partial r} dr' = -\int \frac{r - r't}{L^3} dr' = -\frac{r'}{rL} + C \tag{5.9}$$

The singular value for the effect on gravity disturbance is:

$$\delta g^R|_0 = \frac{1}{2} G\rho \sqrt{\pi A_0}\left(h_x^2 + h_y^2\right) \tag{5.10}$$

where $\left(h_x, h_y\right)$ is the terrain slope vector at the computation point.

Vertical Deflections: Using spherical trigonometry relations for $\partial\psi/\partial\varphi = -cos\alpha$ and $\partial\psi/\partial\lambda = -cos\varphi sin\alpha$, the local terrain effect on vertical deflection vector (ξ^R, η^R) are:

$$\xi^R = -\frac{\partial T^R}{\gamma r \partial\varphi} = -\frac{\partial T^R}{\gamma r \partial\psi}\frac{\partial\psi}{\partial\varphi} = \frac{\partial T^R}{\gamma r \partial\psi} cos\alpha$$

$$= \frac{G\rho}{\gamma r}\iint_S \int_{R+h}^{R+h'} \frac{\partial L^{-1}(r,\psi,r')}{\partial \psi} dr' cos\alpha ds \quad (5.11)$$

$$\eta^R = -\frac{\partial T^R}{\gamma r cos\varphi \partial \lambda} = -\frac{\partial T^R}{\gamma r cos\varphi \partial \psi}\frac{\partial \psi}{\partial \lambda} = \frac{\partial T^R}{\gamma r cos\varphi \partial \psi} cos\varphi sin\alpha$$

$$= \frac{G\rho}{\gamma r}\iint_S \int_{R+h}^{R+h'} \frac{\partial L^{-1}(r,\psi,r')}{\partial \psi} dr' sin\alpha ds \quad (5.12)$$

where α is the geodetic azimuth of ψ, and

$$\int \frac{\partial L^{-1}(r,\psi,r')}{\partial \psi} dr' = \frac{r - r't}{L sin\psi} + C \quad (5.13)$$

From spherical trigonometry formulas:

$$sin\psi cos\alpha = cos\varphi sin\varphi' - sin\varphi cos\varphi' cos(\lambda' - \lambda) \quad (5.14)$$

$$sin\psi sin\alpha = cos\varphi' sin(\lambda' - \lambda) \quad (5.15)$$

Gravity Gradients: The radial component T_{rr}^R is given by:

$$T_{rr}^R = \frac{\partial^2}{\partial r^2} T^R = G\rho \iint_S \int_{R+h}^{R+h'} \frac{\partial^2 L^{-1}(r,\psi,r')}{\partial r^2} dr'\, ds \quad (5.16)$$

with the inner integral:

$$\int \frac{\partial^2 L^{-1}(r,\psi,r')}{\partial r^2} dr' = \int \left[-\frac{1}{L^3} + \frac{3(r - r't)^2}{L^5}\right] dr' = \frac{r'}{r^2 L} + \frac{r'(r - r't)}{rL^3} + C \quad (5.17)$$

Similarly, The tangential components (T_{nn}^R, T_{ww}^R) are derived via chain rules involving second derivatives with respect to ψ.

$$T_{nn}^R = \frac{1}{r^2} T_{\varphi\varphi}^R \quad (5.18)$$

$$T_{ww}^R = -\frac{1}{r^2 cos^2\varphi} T_{\lambda\lambda}^R \quad (5.19)$$

where,

$$T_{\varphi\varphi}^R = \frac{\partial^2 T^R}{\partial \psi^2}\frac{\partial^2 \psi}{\partial \varphi^2}, \quad T_{\lambda\lambda}^R = \frac{\partial^2 T^R}{\partial \psi^2}\frac{\partial^2 \psi}{\partial \lambda^2} \quad (5.20)$$

Taking the partial derivative of both sides of Eq. 5.14 with respect to φ:

$$-cos\psi cos^2\alpha + sin\psi \frac{\partial^2 \psi}{\partial \varphi^2} = -\sin\varphi sin\varphi' - cos\varphi cos\varphi' cos(\lambda' - \lambda) \quad (5.21)$$

Thus,

$$sin\psi \frac{\partial^2 \psi}{\partial \varphi^2} = -\sin\varphi sin\varphi' - cos\varphi cos\varphi' cos(\lambda' - \lambda) + cos\psi cos^2\alpha \quad (5.22)$$

Taking the partial derivative of both sides of Eq. 5.15 with respect to λ:

$$-cos\psi cos\varphi sin^2\alpha + sin\psi \frac{\partial^2 \psi}{\partial \lambda^2} = -cos\varphi' sin(\lambda' - \lambda) \quad (5.23)$$

Thus,

$$sin\psi \frac{\partial^2 \psi}{\partial \lambda^2} = -cos\varphi' sin(\lambda' - \lambda) + cos\psi cos\varphi sin^2\alpha \quad (5.24)$$

Taking the second partial derivative of both sides of the integral expression for the local terrain effect on the disturbing potential Eq. 5.5 with respect to the spherical angle distance ψ:

$$\frac{\partial^2 T^R}{\partial \psi^2} = G\rho \iint_S \int_{R+h}^{R+h'} \frac{\partial^2}{\partial \psi^2}\frac{1}{L} dr' ds =$$

$$G\rho \iint_S \int_{R+h}^{R+h'} \frac{\partial^2}{\partial \psi^2} \frac{1}{\sqrt{r^2 + r'^2 - 2rr' cos\psi}} dr' ds \quad (5.25)$$

where:

$$\int \frac{\partial^2}{\partial\psi^2}\frac{1}{L}dr' = \frac{r'(6r^2+4r'^2+6r^2cos2\psi-rr'cos3\psi)-rt(4r^2+11r'^2)}{4L^3sin^2\psi} \tag{5.26}$$

Physical Remarks:

- The topographic mass effect on gravity disturbance equals the effect on gravity itself.
- In high-altitude regions, local terrain effects on gravity can be positive or negative.
- These effects are non-zero in coastal zones but vanish in the deep ocean.

(2) Fast Algorithm for Local Terrain Effect Integrals

A Local Horizontal Polar Coordinate System is established with the z-axis directed toward the zenith and the origin O located on the terrain surface directly beneath the computation point. At the origin, $z = 0$. Let $\tilde{h}$ denote the elevation of the computation point relative to the underlying terrain surface O. In this local coordinate system, $dz = dr'$ and $d\tilde{h} = dr$, as illustrated in Figure 7.5. The rigorous integral for the local terrain effect on the disturbing potential Eq. (5.5) transforms into:

$$T^R = G\rho \iint_s \int_0^{\Delta h}\frac{dz}{L}ds = G\rho \iint_s \int_0^{\Delta h}\frac{dz}{\sqrt{(\tilde{h}-z)^2+l^2}}ds$$
$$= G\rho \iint_s \left[ln\frac{\sqrt{(\tilde{h}-\Delta h)^2+l^2}-\tilde{h}+\Delta h}{\sqrt{(\tilde{h}-\Delta h)^2+l^2}+\tilde{h}-\Delta h} - ln\frac{\sqrt{\tilde{h}^2+l^2}-H}{\sqrt{\tilde{h}^2+l^2}+H}\right]ds \tag{5.27}$$

where:

Δh: Height difference of the integration area element ds relative to the terrain surface O directly beneath the computation point.

l: Planar distance from the area element ds to point O on the equielevation surface passing through O.

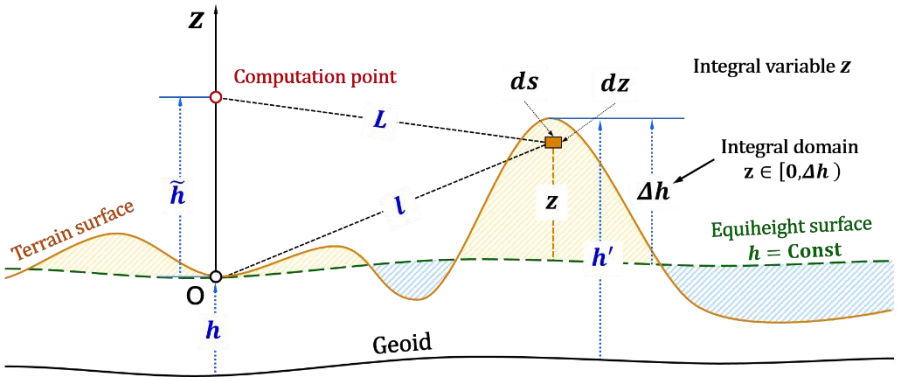

Figure 7.5: Geometric relationships of elements in the rigorous integral for local terrain effects within the local polar coordinate system.

Since the rigor of gravity field integrals depends solely on the accurate calculation of the area element and its spatial distance to the computation point, Eq. (5.27) is mathematically equivalent to Eq. (5.5) and constitutes a rigorous formulation. Expanding the integrand of Eq. (5.27) in a Taylor series around $z = 0$ up to the third order yields:

$$T^R = G\rho \iint_s \left[\frac{1}{\mathcal{L}}\Delta h + \frac{\tilde{h}}{2\mathcal{L}^3}\Delta h^2 + \frac{2\tilde{h}^2-l^2}{6\mathcal{L}^5}\Delta h^3\right]ds \tag{5.28}$$

Here, $\mathcal{L} = \sqrt{\tilde{h}^2 + l^2}$ represents the spatial distance from the surface element ds (at $z = 0$) to the external computation point. Note that this $\mathcal{L}$ differs from the distance involving the volume

element $dzds$.

By substituting the binomial expansions $\Delta h^k = (h' - h)^k$ (where h' is the terrain elevation at ds and h is the elevation at 0), each term inside the integral assumes a convolution form dependent only on the integration variable l (embedded in $\mathcal{L}$) and the terrain elevations. Consequently, the Fast Fourier Transform (FFT) algorithm can be applied term-by-term for rapid computation.

Similarly, the rigorous integral for the local terrain effect on the gravity disturbance (Eq. 5.8) becomes:

$$\delta g^R = \frac{G\rho}{r}\iint_S \left[\frac{(r_0+z)}{\sqrt{(\tilde{h}-z)^2+l^2}}\right]_0^{\Delta h} ds = \frac{G\rho}{r}\iint_S \left[\frac{r_0+\Delta h}{\sqrt{(\tilde{h}-\Delta h)^2+l^2}} - \frac{r_0}{\mathcal{L}}\right] ds \tag{5.29}$$

Expanding the integrand around $z = 0$ up to the fourth order:

$$\delta g^R = \frac{G\rho}{r}\iint_S \left[\begin{matrix} \frac{r\tilde{h}+\mathcal{L}^2}{\mathcal{L}^3}\Delta h + \frac{2\tilde{h}\mathcal{L}^2+r_0(2\tilde{h}^2-l^2)}{2\mathcal{L}^5}\Delta h^2 + \frac{2\tilde{h}^3 r+\tilde{h}^2 l^2-3r_0\tilde{h}l^2-l^4}{2\mathcal{L}^7} \\ \Delta h^3 + \frac{8r\tilde{h}^4-4\tilde{h}^3 l^2-12\tilde{h}l^4-24r_0\tilde{h}^2 l^2+3l^4 r_0}{8\mathcal{L}^9}\Delta h^4 \end{matrix}\right] ds \tag{5.30}$$

Equation (5.30) is also amenable to FFT acceleration after expansion.

For the vertical deflection, expanding the integrand up to the third order yields the kernel:

$$-\frac{r^2 sin\psi}{\mathcal{L}^3}\Delta h - \frac{3\tilde{h}r^2 sin\psi}{2\mathcal{L}^5}\Delta h^2 - \left[\frac{r^2 sin\psi}{3\mathcal{L}^5} + \frac{5r^2 sin\psi(2\tilde{h}^2-l^2)}{6\mathcal{L}^7}\right]\Delta h^3 \tag{5.31}$$

Substituting Eq. (5.31) into Eqs. (5.11) and (5.12) enables fast FFT-based computation of the local terrain effect on vertical deflections.

For the disturbing gravity gradient (T_{rr}^R), the equivalent rigorous integral is:

$$T_{rr}^R = G\rho\iint_S \left[\frac{\tilde{h}-\Delta h}{((\tilde{h}-\Delta h)^2+l^2)^{3/2}} - \frac{\tilde{h}}{\mathcal{L}^3}\right] ds \tag{5.32}$$

Expanding up to the third order:

$$T_{rr}^R = G\rho\iint_S \left[\begin{matrix} \frac{2\tilde{h}^2-l^2}{\mathcal{L}^5}\Delta h - \frac{3\tilde{h}(2\tilde{h}^2-3l^2)}{2\mathcal{L}^7}\Delta h^2 + \\ \frac{4\tilde{h}^4+6r^4-12\tilde{h}^2 l^2-(6r^4+3r^2 l^2)cos\psi}{\mathcal{L}^9}\Delta h^3 \end{matrix}\right] ds \tag{5.33}$$

The integrand in the rigorous integral expression for the local terrain effect on the tangential gravity gradient (Equation 5.25) is equivalent to:

$$\begin{aligned}\int_{R+h}^{R+h'} \frac{\partial^2}{\partial\psi^2}\frac{1}{L}dr' &= \int_0^{\Delta h}\frac{\partial^2}{\partial\psi^2}\frac{1}{\sqrt{(\tilde{h}-z)^2+4r_0^2 sin^2(\psi/2)}}dz \\ &= \frac{1}{8sin^2\frac{\psi}{2}}\left[\frac{\tilde{h}(2\mathcal{L}^2+r_0^2 sin^2\psi)}{\mathcal{L}^3} - \frac{(\tilde{h}-\Delta h)(2\mathcal{L}^2+r_0^2 sin^2\psi-4\tilde{h}\Delta h+2\Delta h^2)}{(\mathcal{L}^2-2\tilde{h}\Delta h+\Delta h^2)^{3/2}}\right]\end{aligned} \tag{5.34}$$

Expanding around $z = 0$ up to the third order yields:

$$\begin{aligned}\int_{R+h}^{R+h'} \frac{\partial^2}{\partial\psi^2}\frac{1}{L}dr' &= -\frac{2(\tilde{h}^2+2r_0^2)cos\psi+r_0^2(-5+cos2\psi)}{2L^5}r_0^2\Delta h \\ &+ \frac{6(\tilde{h}^2+2r_0^2)cos\psi+3r_0^2(-7+3cos2\psi)}{4\mathcal{L}^7}\tilde{h}r_0^2\Delta h^2 \\ &+ \frac{(8\tilde{h}^4+12\tilde{h}^2 r_0^2-19r_0^4)cos\psi-r_0^2(36\tilde{h}^2-18r_0^2-(24\tilde{h}^2-2r_0^2)cos2\psi+3r_0^2 cos3\psi)}{4\mathcal{L}^9}r_0^2\Delta h^3\end{aligned} \tag{5.35}$$

If the computation point lies on the terrain surface ($\tilde{h} = 0$, $\mathcal{L} = l$), Eqs. (5.27) – (5.35) simplify significantly.

7.5.3 Integral Algorithm for Land-Sea Complete Bouguer Effects outside the Geoid

In oceanic regions, the topographic gravitational field is modeled as the Seawater Complete Bouguer Effect, defined as the effect resulting from compensating the seawater density (ρ_w) to the land topographic density (ρ).

The rigorous integral for the Seawater Complete Bouguer Effect on the disturbing potential is:

$$T^o = G\beta \iint_s \int_{R+d}^{R} L^{-1}(r,\psi,r')\, dr'\, ds \tag{5.36}$$

where:

$d < 0$: Bathymetry (sea depth) relative to mean sea level.

$\beta = \rho - \rho_w$ =1.64×10³kg/m^3: Seawater compensation density.

L : Spatial distance from the seawater volume element to the computation point.

Using the local horizontal polar coordinate system (z -axis points toward the zenith, $z = 0$ at sea surface), Eq. (5.36) becomes:

$$T^o = G\beta \iint_s \int_d^0 \frac{dz}{L} ds = G\beta \iint_s \int_d^0 \frac{dz}{\sqrt{(\tilde{h}-z)^2+l^2}} ds$$

$$= G\beta \iint_s \left[ln\frac{\sqrt{\tilde{h}^2+l^2}-\tilde{h}}{\sqrt{\tilde{h}^2+l^2}+\tilde{h}} - ln\frac{\sqrt{(\tilde{h}-d)^2+l^2}-\tilde{h}+d}{\sqrt{(\tilde{h}-d)^2+l^2}+\tilde{h}-d} \right] ds \tag{5.37}$$

where $l = 2r_0 \sin(\psi/2)$ is the planar distance on the sea surface, $\tilde{h}$ is the computation point's altitude, and r_0 is the mean geocentric distance of the sea surface.

Similarly, the rigorous integral expression for the seawater complete Bouguer effect on on the gravity disturbance is:

$$\delta g^o = -\frac{\partial T^o}{\partial r} = -G\beta \iint_s \int_{R+d}^{R} \frac{\partial L^{-1}(r,\psi,r')}{\partial r} dr'\, ds \tag{5.38}$$

which is equivalent to:

$$\delta g^o = \frac{G}{r} \iint_s \beta \int_d^0 \frac{(r_0+z)dz}{\sqrt{(\tilde{h}-z)^2+l^2}} ds = \frac{G\beta}{r} \iint_s \left[\frac{r_0}{\mathcal{L}} - \frac{r_0+d}{\sqrt{(\tilde{h}-d)^2+l^2}} \right] ds \tag{5.39}$$

The rigorous integral expressions for the seawater complete Bouguer effect on the vertical deflection are:

$$\xi^o = \frac{T_\theta^o}{\gamma r} = \frac{G\beta}{\gamma r} \iint_s \int_{R+d}^{R} \frac{\partial L^{-1}(r,\psi,r')}{\partial \psi} dr' cos\alpha ds \tag{5.40}$$

$$\eta^o = -\frac{T_\lambda^o}{\gamma r sin\theta} = \frac{G\beta}{\gamma r} \iint_s \int_{R+d}^{R} \frac{\partial L^{-1}(r,\psi,r')}{\partial \psi} dr' sin\alpha ds \tag{5.41}$$

The rigorous integral expression for the complete Bouguer effect of seawater on the disturbing gravity gradient is:

$$T_{rr}^o = \frac{\partial^2}{\partial r^2} T^o = G\beta \iint_s \int_{R+d}^{R} \frac{\partial^2 L^{-1}(r,\psi,r')}{\partial r^2} dr'\, ds \tag{5.42}$$

which is equivalent to:

$$T_{rr}^o = G\beta \iint_s \left[\frac{\tilde{h}-d}{((\tilde{h}-d)^2+l^2)^{3/2}} - \frac{h}{\mathcal{L}^3} \right] ds \tag{5.43}$$

FFT Acceleration:

By expanding the integrands of Eqs. (5.37), (5.39), (5.40 – 41), and (5.43) in Taylor series around the sea surface (z = 0), we obtain convolution forms suitable for FFT. For

example, the expansion for T^o up to the third order is:

$$T^o = G\beta \int_d^0 \frac{1}{L} dzds = G\beta \iint_s \left(\frac{1}{\mathcal{L}} d + \frac{\tilde{h}}{2\mathcal{L}^3} d^2 + \frac{2\tilde{h}^2 - l^2}{6\mathcal{L}^5} d^3\right) ds \tag{5.44}$$

Similar expansions for δg^0 (4th order), vertical deflections (3rd order), and T_{rr}^o (3rd order) are provided in Eqs. (5.45) – (5.47). All expanded terms can be computed efficiently using the FFT algorithm.

$$\delta g^0 = \frac{G}{r} \iint_s \beta \left[\begin{array}{c} \frac{r\tilde{h}+\mathcal{L}^2}{\mathcal{L}^3} d + \frac{2\tilde{h}\mathcal{L}^2 + r_0(\tilde{h}^2+\mathcal{L}^2)}{2\mathcal{L}^5} d^2 + \frac{2\tilde{h}^3 r + \tilde{h}^2 l^2 - 3r_0\tilde{h}l^2 - l^4}{2\mathcal{L}^7} \\ d^3 + \frac{8r\tilde{h}^4 - 4\tilde{h}^3 l^2 - 12\tilde{h}l^4 - 24r_0\tilde{h}^2 l^2 + 3l^4 r_0}{8\mathcal{L}^9} d^4 \end{array}\right] ds \tag{5.45}$$

$$\int_{R+d}^{R} \frac{\partial L^{-1}(r,\psi,r')}{\partial \psi} dr'$$

$$= -\frac{r^2 sin\psi}{\mathcal{L}^3} d - \frac{3\tilde{h}r^2 sin\psi}{2\mathcal{L}^5} d^2 - \left[\frac{r^2 sin\psi}{3\mathcal{L}^5} + \frac{5r^2 sin\psi(2\tilde{h}^2 - l^2)}{6\mathcal{L}^7}\right] d^3 \tag{5.46}$$

$$T_{rr}^o = -\frac{\partial \delta g^o}{\partial r} = G\beta \iint_s \left[\begin{array}{c} \frac{2\tilde{h}^2 - l^2}{\mathcal{L}^5} d + \frac{3\tilde{h}(2\tilde{h}^2 - 3l^2)}{2\mathcal{L}^7} d^2 + \\ \frac{4\tilde{h}^4 + 6r^4 - 12\tilde{h}^2 l^2 - (6r^4 + 3r^2 l^2) cos\psi}{\mathcal{L}^9} d^3 \end{array}\right] ds \tag{5.47}$$

Simplification: If the computation point is on the sea surface ($h = 0$, $\mathcal{L} = l$), all equations simplify considerably.

Magnitude and Computational Strategy for Seawater Complete Bouguer Effects

The magnitude of the Seawater Complete Bouguer Effect on various external gravity field elements is substantial. In practical computations, a sufficiently large integration radius (e.g., ≥250 km) is required to capture these effects accurately. Coastal land areas are influenced by the seawater Bouguer effect, while nearshore waters are affected by the local terrain effect of adjacent land masses. Consequently, the coastal transition zone is subject to both effects simultaneously.

Given the significant magnitude of Spherical Shell Bouguer Effects, approximating topographic reliefs solely via third-order Taylor expansions can introduce errors exceeding the gravity disturbance signal itself in certain regions. Therefore, it is strongly recommended that:

- The Complete Bouguer effect only on gravity may be computed using direct integral methods.
- The Complete Bouguer effects on all other gravity field elements (including gravity, if highest precision is required) should be computed using the Remove-Restore technique. This involves computing the Residual Terrain Effect (RTE) via rigorous integrals, using a global land-sea topographic mass model represented by spherical harmonic coefficients as the reference field.

7.5.4 Integral Algorithms for Residual Terrain Effects (RTE) outside the Geoid

The Land-Sea Residual Terrain Effect is defined as the short- and ultra-short-wavelength components of the Land-Sea Complete Bouguer Effect. The computational workflow involves:

- Constructing a Residual Terrain Model (RTM) by subtracting a low-pass filtered terrain grid from a high-resolution terrain grid (both with identical specifications).
- Computing the effects of this RTM on various field elements using rigorous integral

formulas.

The integral formulations for RTE are formally identical to those for local terrain and seawater Bouguer effects, differing only in the density parameter (β') and the radial integration limits defined by the residual elevation/ bathymetry (δ').

The RTE on the disturbing potential in external space is:

$$T^{\mathrm{rtm}} = G \iint_s \int_R^{R+\delta'} \beta' L^{-1}(r,\psi,r')\, dr'\, ds \tag{5.48}$$

where:

δ': Residual terrain elevation (land) or residual bathymetry (ocean). Note that δ' can be positive or negative.

β': Density parameter. That is topographic density ρ (land) or seawater compensation density $\beta' = \rho - \rho_w$ (ocean).

Similarly, the RTE on other field elements are:

● Gravity Disturbance:

$$\delta g^{\mathrm{rtm}} = -\frac{\partial T^{\mathrm{rtm}}}{\partial r} = -G \iint_s \beta' \int_R^{R+\delta'} \frac{\partial L^{-1}(r,\psi,r')}{\partial r} dr'\, ds \tag{5.49}$$

● Vertical Deflections:

$$\xi^{\mathrm{rtm}} = \frac{G}{\gamma r} \iint_s \beta' \int_R^{R+\delta'} \frac{\partial L^{-1}(r,\psi,r')}{\partial \psi} dr' cos\alpha ds \tag{5.50}$$

$$\eta^{\mathrm{rtm}} = \frac{G}{\gamma r} \iint_s \beta' \int_R^{R+\delta'} \frac{\partial L^{-1}(r,\psi,r')}{\partial \psi} dr' sin\alpha ds \tag{5.51}$$

● Radial Gravity Gradient:

$$T_{rr}^{\mathrm{rtm}} = \frac{\partial^2}{\partial r^2} T^{\mathrm{rtm}} = G \iint_s \beta' \int_R^{R+\delta'} \frac{\partial^2 L^{-1}(r,\psi,r')}{\partial r^2} dr'\, ds \tag{5.52}$$

Rigorous Integral Formulations within a Local Coordinate System:

Adopting a Local Horizontal Polar Coordinate System ($z = 0$ at the surface, z-axis to zenith), let $\mathcal{L} = \sqrt{\tilde{h}^2 + l^2}$ be the distance from the surface element to the computation point. The rigorous integrals can be rewritten in closed form:

● RTE on disturbing Potential:

$$T^{\mathrm{rtm}} = G \iint_s \beta' \int_0^{\delta'} \frac{dz}{\sqrt{(\tilde{h}-z)^2 + l^2}} ds$$

$$= G \iint_s \beta' \left[ln \frac{\sqrt{(\tilde{h}-\delta')^2 + l^2} - \tilde{h} + \delta'}{\mathcal{L} + \tilde{h} - \delta'} - ln \frac{\mathcal{L} - \tilde{h}}{\mathcal{L} + \tilde{h}} \right] ds \tag{5.53}$$

● RTE on Gravity Disturbance:

$$\delta g^{\mathrm{rtm}} = \frac{G}{r} \iint_s \beta' \iint_0^{\Delta h} \frac{\partial}{\partial \tilde{h}} \frac{dz}{\sqrt{(\tilde{h}-z)^2 + l^2}} ds = \frac{G}{r} \iint_s \beta' \left[\frac{1}{\sqrt{(\tilde{h}-\Delta h)^2 + l^2}} - \frac{1}{\mathcal{L}} \right] ds \tag{5.54}$$

● RTE on vertical deflection (Kernel expansion):

$$\int_R^{R+\delta'} \frac{\partial L^{-1}(r,\psi,r')}{\partial \psi} dr' = \frac{1}{2} ctg \frac{\psi}{2} \left[\frac{\tilde{h} - \delta'}{\sqrt{(\tilde{h}-\delta')^2 + l^2}} - \frac{\tilde{h}}{\mathcal{L}} \right] \tag{5.55}$$

● RTE on Radial Gravity Gradient:

$$T_{rr}^{\mathrm{rtm}} = G\iint_s \beta'\left[\frac{\tilde{h}-\delta'}{((\tilde{h}-\delta')^2+l^2)^{3/2}} - \frac{\tilde{h}}{\mathcal{L}^3}\right] ds \tag{5.56}$$

Fast Computation via Taylor Expansion:

Expanded in a Taylor series around $z = 0$ to derive convolution forms suitable for FFT acceleration:

To enable fast computation, the integrands in the above rigorous integral expressions are expanded around $z = 0$, which here represents the land terrain / sea surface. Expanding the integrand in Equation (5.53) around $z = 0$ yields:

● Disturbing Potential (3rd order):

$$T^{\mathrm{rtm}} = -G\iint_s \beta'\left(\frac{1}{\mathcal{L}}\delta' + \frac{\tilde{h}}{2\mathcal{L}^3}\delta'^2 + \frac{2\tilde{h}^2-l^2}{6\mathcal{L}^5}\delta'^3\right) ds \tag{5.57}$$

● Gravity Disturbance (4th order):

$$\delta g^{\mathrm{rtm}} = \frac{G}{r}\iint_s \beta'\left[\frac{\tilde{h}}{\mathcal{L}^3}\delta' + \frac{2\tilde{h}^2-l^2}{2\mathcal{L}^5}\delta'^2 + \frac{\tilde{h}(2\tilde{h}^2-3l^2)}{2\mathcal{L}^7}\delta'^3 + \frac{8\tilde{h}^4-24\tilde{h}^2l^2+3l^4}{8\mathcal{L}^9}\delta'^4\right] ds \tag{5.58}$$

● Vertical Deflections (Kernel expansion, 3rd order):

$$\int_R^{R+\delta'} \frac{\partial L^{-1}(r,\psi,r')}{\partial\psi} dr' = -\frac{r^2 sin\psi}{\mathcal{L}^3}\delta' - \frac{3\tilde{h}r^2 sin\psi}{2\mathcal{L}^5}\delta'^2 - \left[\frac{r^2 sin\psi}{3\mathcal{L}^5} + \frac{5r^2 sin\psi(2\tilde{h}^2-l^2)}{6\mathcal{L}^7}\right]\delta'^3 \tag{5.59}$$

● Radial Gravity Gradient (4th order):

$$T_{rr}^{\mathrm{rtm}} = G\iint_s \beta'\left[\frac{2\tilde{h}^2-l^2}{\mathcal{L}^5}\delta' + \frac{3\tilde{h}(2\tilde{h}^2-3l^2)}{2\mathcal{L}^7}\delta'^2 + \frac{8\tilde{h}^4-24\tilde{h}^2l^2+3l^4}{2\mathcal{L}^9}\delta'^3\right] ds \tag{5.60}$$

These expanded terms depend only on the residual elevation powers (δ'^k) and the geometric kernel ($\mathcal{L}$, l , $\tilde{h}$), allowing for efficient evaluation using the Fast Fourier Transform (FFT) algorithm.

7.6 Local Terrain Compensation and Terrain Helmert Condensation

7.6.1 Effects of Terrain Helmert Condensation on Gravity Field elements

The Helmert condensation of topographic masses is based on the concept of topographic mass compensation (referred to henceforth as terrain compensation). For any gravity field element defined on or outside the geoid, terrain compensation is defined as the mass adjustment applied to counteract the gravitational field changes induced by the removal of topographic masses.

The process of Terrain Helmert Condensation comprises two distinct steps:

● Removal: Subtract the gravitational field generated by the actual topographic masses (i.e., subtract the Land Complete Bouguer Effect).

● Compensation: Add the gravitational field generated by the condensed mass layer to compensate for the removal (i.e., add the Terrain Compensation).

The net change in any external gravity field element α due to this process is termed the Terrain Helmert Condensation Effect, expressed uniformly as:

$$\alpha^h = \alpha^t - \alpha^c \tag{6.1}$$

where:

α^h: Terrain Helmert condensation effect on α.

α^t: Land Complete Bouguer effect on α.

α^c: Terrain compensation effect on α.

Unlike local terrain or complete Bouguer effects, Helmert condensation preserves the total topographic masses. Consequently, the vertical component of the Helmert condensation effect is generally significantly smaller than both the complete Bouguer effect and the local terrain effect.

The space external to the geoid after this transformation is referred to as Helmert Space, and the resulting field is the Helmert Gravity Field. This field differs from the actual Earth's gravity field solely by the harmonic field change induced by the condensation. Notably, the terrain Helmert condensation effect retains the harmonic property in external space.

7.6.2 Algorithms for Terrain Compensation and Helmert Condensation Effects

This section introduces the algorithms for computing terrain compensation on various gravity field elements at arbitrary altitudes within the near-Earth harmonic space.

● Disturbing Potential:

The terrain compensation effect on the external disturbing potential is defined as:

$$T^c = T^B + T^{cR} = T^B + G\iint_s \frac{\mu'-\mu}{L} ds \tag{6.2}$$

where:

T^{cR}: Local Terrain Compensation on the disturbing potential.

ds: Moving area element on the terrain surface.

μ: Topographic mass compensation density. Under spherical approximation:

$$\mu = \rho h\left(1 + \frac{h}{R} + \frac{h^2}{3R^2}\right) \tag{6.3}$$

where h is the ground elevation directly beneath the computation point, and ρ is the topographic density.

By approximating the geocentric distances with mean values for the computaion surface and terrain surfaces, the integral term in Eq. (6.2) can be computed efficiently using the Fast Fourier Transform (FFT) algorithm.

Singularity Handling: When the computation point coincides with the integration moving point, T^{cR} becomes singular. The analytical value of this singular integral is:

$$T^{cR}|_0 = \frac{R^2}{6\tilde{r}^2} G A_0 \sqrt{A_0/\pi}\left(\mu_{xx} + \mu_{yy}\right) \tag{6.4}$$

where μ_{xx}, μ_{yy} are the second-order partial derivatives of the topographic mass compensation density at the computation point in the north (x) and east (y) directions, respectively.

● Gravity Disturbance:

Substituting Eq. (6.2) into the definition of gravity disturbance yields:

$$\delta g^c = \delta g^B + \delta g^{cR} = \delta g^B + G\iint_s (\mu' - \mu)\frac{r - r't}{L^3} ds \tag{6.5}$$

where δg^{cR} is the local terrain compensation effect on the gravity disturbance. Its singular value is:

$$\delta g^{cR}|_0 = \frac{R^2}{12\tilde{r}^3} G A_0 \sqrt{A_0/\pi}\left(\mu_{xx} + \mu_{yy}\right) \tag{6.6}$$

● General Formulation:

Combining Eqs. (6.2) and (6.5), the Terrain Helmert Condensation effect for any field element α simplifies to:

$$\alpha^h = \alpha^t - \alpha^c = (\alpha^B + \alpha^R) - (\alpha^B + \alpha^{cR}) = \alpha^R - \alpha^{cR} \tag{6.7}$$

Under spherical approximation, the Spherical Shell Bouguer effect (α^B) cancels out. Thus, the Helmert condensation effect is simply the difference between the Local Terrain Effect (α^R) and the Local Terrain Compensation (α^{cR}).

● FFT Implementation Details:

Adopting a Local Horizontal Polar Coordinate System (z-axis to zenith, $dr = d\tilde{h}$), the local terrain compensation on gravity disturbance can be expanded into convolution terms suitable for FFT:

$$\begin{aligned}\delta g^{cR} = -G\iint_S (\mu' - \mu)\frac{\partial}{\partial \tilde{h}}\frac{1}{L}ds &= G\iint_S (\mu' - \mu)\frac{\tilde{h}}{L^3} - \frac{\mu' - \mu}{L^3}(h' - h)ds \\ &= G\iint_S (\mu' - \mu)\frac{\tilde{h}}{L^3}ds - G\iint_S \frac{\mu' h'}{L^3}\frac{t}{L}ds \\ &+ G\iint_S \frac{\mu' h}{L^3}ds + G\iint_S \frac{\mu h'}{L^3}ds - G\iint_S \frac{\mu h}{L^3}ds\end{aligned} \tag{6.8}$$

Note: Eq. 6.8 decomposes the integrand into separate convolutions of compensation densities and geometric kernels, all computable via FFT.

Similarly, using the relation:

$$\frac{\partial L^{-1}(r,\psi,r')}{\partial \psi} = \frac{rr'sin\psi}{L^3}, \quad \frac{\partial \psi}{\partial \varphi} = -cos\alpha, \quad \frac{\partial \psi}{\partial \lambda} = -cos\varphi sin\alpha \tag{6.9}$$

the FFT formulas for Vertical Deflections are:

$$\begin{aligned}\xi^{cR} = -\frac{\partial T^{cR}}{\gamma r \partial \varphi} = -\frac{\partial T^{cR}}{\gamma r \partial \psi}\frac{\partial \psi}{\partial \varphi} = \frac{\partial T^{cR}}{\gamma r \partial \psi}cos\alpha &= \frac{G}{\gamma r}\iint_S (\mu' - \mu)\frac{\partial L^{-1}(r,\psi,r')}{\partial \psi}cos\alpha ds \\ &= \frac{G}{\gamma}\int_S (\mu' - \mu)\frac{r' sin\psi}{L^3}cos\alpha ds\end{aligned} \tag{6.10}$$

$$\begin{aligned}\eta^{cR} = -\frac{\partial T^{cR}}{\gamma r cos\varphi \partial \psi}\frac{\partial \psi}{\partial \lambda} = \frac{\partial T^{cR}}{\gamma r \partial \psi}sin\alpha &= \frac{G}{\gamma r}\iint_S \frac{\partial L^{-1}(r,\psi,r')}{\partial \psi}(\mu' - \mu)sin\alpha ds \\ &= \frac{G}{\gamma}\iint_S (\mu' - \mu)\frac{r' sin\psi}{L^3}sin\alpha ds\end{aligned} \tag{6.11}$$

And for the Radial Gravity Gradient:

$$\begin{aligned}T_{rr}^{cR} = \frac{\partial^2}{\partial r^2}T^{cR} = G\iint_S (\mu' - \mu)\frac{\partial^2}{\partial r^2}\left(\frac{1}{L}\right)ds \\ = G\iint_S (\mu' - \mu)\left(3\frac{r - r'cos\psi}{L^5} - \frac{1}{L^3}\right)ds\end{aligned} \tag{6.12}$$

Equations (6.10) through (6.12) provide the rigorous kernel functions required for FFT-based computation of local terrain compensation effects on vertical deflections and gravity gradients.

7.7 Spherical Harmonic Analysis and Synthesis of Land-Sea Terrain Masses

The terrain surface density $q(\theta, \lambda)$ at any point P(θ, λ, R) on the land or sea surface can be expanded in terms of normalized spherical harmonic coefficients as:

$$q(\theta,\lambda) = \beta h = a\sum_{n=1}^{\infty}\sum_{m=0}^{n}[A_{nm}cosm\lambda + B_{nm}sinm\lambda]\,\bar{P}_{nm}(cos\theta) \tag{7.1}$$

where:

a: Semi-major axis of the Earth's ellipsoid (used for consistency with global

geopotential model).

A_{nm}, B_{nm}: Normalized spherical harmonic coefficients of the topographic mass of degree n and order m.

$\bar{P}_{nm}$: Fully normalized associated Legendre functions.

Parameters:

- On land: $h > 0$ is the terrain elevation, and $\beta = \rho = 2.67\times10^3$kg/m^3 is the topographic density.
- On sea: $h <$ is the bathymetry, and $\beta = \rho - \rho_w = 1.64\times10^3$kg/m^3 is the seawater compensation density.

The Land-Sea Complete Bouguer Effect on the geopotential at an external point (θ, λ, r) is expressed via the global terrain mass spherical harmonic series:

$$V^{\mathrm{tbg}}(\theta,\lambda,r) = \frac{3GM}{r\rho_e}\sum_{n=1}^{\infty}\left(\frac{a}{r}\right)^n \sum_{m=0}^{n}(A_{nm}cosm\lambda + B_{nm}sinm\lambda)\bar{P}_{nm}(cos\theta) \tag{7.2}$$

where $\rho_e = 5.517\times10^3$kg/m^3 is the Earth's mean density.

The Residual Terrain Effect (RTE) on the geopotential is obtained by truncating the series at a minimum degree n_1:

$$V^{\mathrm{rtm}}(\theta,\lambda,r) = \frac{3GM}{r\rho_e}\sum_{n=n_1}^{\infty}\left(\frac{a}{r}\right)^n \sum_{m=0}^{n}(A_{nm}cosm\lambda + B_{nm}sinm\lambda)\bar{P}_{nm}(cos\theta) \tag{7.3}$$

The relationship between the normalized terrain mass coefficients (A_{nm}, B_{nm}) and the normalized terrain gravitational potential coefficients $(\bar{C}^{\mathrm{ter}}_{nm}, \bar{S}^{\mathrm{ter}}_{nm})$ is:

$$\bar{C}^{\mathrm{ter}}_{nm} = \frac{3}{\rho_e}\frac{1}{2n+1}A_{nm}, \quad \bar{S}^{\mathrm{ter}}_{nm} = \frac{3}{\rho_e}\frac{1}{2n+1}B_{nm} \tag{7.4}$$

These coefficients $\bar{C}^{\mathrm{ter}}_{nm}, \bar{S}^{\mathrm{ter}}_{nm}$ represent the Stokes coefficients of the geopotentials generated by the combined land topography and seawater compensation masses. They define the Land-Sea Complete Bouguer Field in the spectral domain.

By substituting Eq. (7.4) into the standard spherical harmonic expansions for anomalous gravity field elements, we derive the synthesis formulas for the Residual Terrain Effects on various gravity field elements in external space:

- Height Anomaly (ζ^{rtm}):

$$\zeta^{\mathrm{rtm}}(\theta,\lambda,r) = \frac{GM}{r\gamma}\frac{3}{\rho_e} \sum_{n=n_1}^{\infty}\left(\frac{a}{r}\right)^n \frac{1}{2n+1}\sum_{m=0}^{n}(A_{nm}cosm\lambda + B_{nm}sinm\lambda)\bar{P}_{nm}(cos\theta) \tag{7.5}$$

- Gravity (Anomaly/Disturbance) (g^{rtm}):

$$g^{\mathrm{rtm}}(\theta,\lambda,r) = \frac{GM}{r^2}\frac{3}{\rho_e}\sum_{n=n_1}^{\infty}\frac{n+1}{2n+1}\left(\frac{a}{r}\right)^n \sum_{m=0}^{n}(A_{nm}cosm\lambda + B_{nm}sinm\lambda)\bar{P}_{nm}(cos\theta) \tag{7.6}$$

- Vertical Deflections ($\xi^{\mathrm{rtm}}, \eta^{\mathrm{rtm}}$):

$$\xi^{\mathrm{rtm}}(\theta,\lambda,r) = \frac{GM}{r^2}\frac{3}{\gamma\rho_e}sin\,\theta\sum_{n=n_1}^{\infty}\frac{1}{2n+1}\left(\frac{a}{r}\right)^n \sum_{m=0}^{n}(A_{nm}cosm\lambda + B_{nm}sinm\lambda)\frac{\partial}{\partial\theta}\bar{P}_{nm}(cos\theta) \tag{7.7}$$

$$\eta^{\mathrm{rtm}}(\theta,\lambda,r) = \frac{GM}{r^2 sin\,\theta}\frac{3}{\gamma\rho_e}\sum_{n=n_1}^{\infty}\frac{1}{2n+1}\left(\frac{a}{r}\right)^n \sum_{m=1}^{n}m(A_{nm}sinm\lambda - B_{nm}cosm\lambda)\bar{P}_{nm}(cos\theta) \tag{7.8}$$

● Radial Gravity Gradient (V_{rr}^{rtm}):

$$V_{rr}^{\mathrm{rtm}}(\theta,\lambda,r) = \frac{GM}{r^3}\frac{3}{\rho_e}\sum_{n=n_1}^{\infty}\frac{(n+1)(n+2)}{2n+1}\left(\frac{a}{r}\right)^n \sum_{m=0}^{n}(A_{nm}cosm\lambda + B_{nm}sinm\lambda)\bar{P}_{nm}(cos\theta) \quad (7.9)$$

● Tangential Gravity Gradients ($V_{nn}^{\mathrm{rtm}}, V_{ww}^{\mathrm{rtm}}$):

$$V_{nn}^{\mathrm{rtm}}(\theta,\lambda,r) = -\frac{GM}{r^3}\frac{3}{\rho_e}\sum_{n=n_1}^{\infty}\frac{1}{2n+1}\left(\frac{a}{r}\right)^n \sum_{m=0}^{n}(A_{nm}cosm\lambda + B_{nm}sinm\lambda)\frac{\partial^2}{\partial\theta^2}\bar{P}_{nm}(cos\theta) \quad (7.10)$$

$$V_{ww}^{\mathrm{rtm}}(\theta,\lambda,r) = -\frac{GM}{r^3 sin^2\theta}\frac{3}{\rho_e}\sum_{n=n_1}^{\infty}\frac{1}{2n+1}\left(\frac{a}{r}\right)^n \sum_{m=1}^{n} m^2(A_{nm}sinm\lambda + B_{nm}cosm\lambda)\bar{P}_{nm}(cos\theta) \quad (7.11)$$

Implementation Notes:

● Setting $n_1 = 1$ yields the formulas for the full Land-Sea Complete Bouguer Effect. The degree-1 term is significant and must be retained.

● For high-precision applications involving short wavelengths, the Remove-Restore technique is recommended: use the spherical harmonic model (Eqs. 7.5 – 7.11) for the long-to-medium wavelengths ($n < n_1$) and rigorous spatial integration (Section 7.5.4) for the residual short wavelengths ($n \geq n_1$).

7.8 Unified Algorithms for Land-Sea Classical Bouguer and Isostatic Effects

7.8.1 Classical Reduction Method for Land Bouguer Gravity Anomalies

The Classical Planar Bouguer Gravity Anomaly is strictly defined on the geoid. It is computed as the gravity anomaly on the geoid minus the gravitational attraction exerted by all topographic masses external to the geoid on the surface gravity. The classical algorithm is expressed as:

$$\Delta g_B = \Delta g - g^R - 2\pi G\rho h \quad (8.1)$$

where:

Δg: Free-air gravity anomaly on the geoid.

$-g^R$: Classical Planar Terrain Correction (g^R represents the planar approximation of the local terrain effect on surface gravity).

$-2\pi G\rho h$: Bouguer Plate Correction ($2\pi G\rho h$ represents the planar approximation of the spherical shell Bouguer effect on surface gravity).

In mountainous regions, the plate correction term is significantly negative, typically resulting in negative Bouguer anomalies. Since observation points are rarely located on the geoid, measured gravity must be analytically continued from the observation attitude down to the geoid to obtain Δg. Only then can Eq. (8.1) be applied.

Thus, the general formula for computing the Planar Bouguer Gravity Anomaly (referenced to the geoid) from ground or airborne observations is:

$$\Delta g_B = \Delta g^s - g^R - 2\pi G\rho h - \Delta g^c \quad (8.2)$$

where Δg^s is the gravity anomaly at the observation point; Δg^c is the analytical continuation term for the gravity anomaly.

Similarly, for the Bouguer Gravity Disturbance:

$$\delta g_B = \delta g^s - g^R - 2\pi G\rho h - \delta g^c \tag{8.3}$$

where: δg^s is the gravity disturbance at the observation point, and $\delta g^c \approx \Delta g^c$.

Critical Implementation Note:

Regardless of whether data are acquired on the ground or from an aircraft, the Bouguer Gravity Anomaly/Disturbance are defined exclusively on the geoid. Furthermore, the topographic correction terms (g^R and the plate correction) specifically represent the effect of topography masses on surface gravity (gravity on the terrain surface), not on gravity at the airborne altitude or on the geoid. Even when processing airborne data, g^R in Eqs. (8.2) and (8.3) must be calculated as the local terrain effect on surface gravity.

7.8.2 Computation of Seawater and Unified Land-Sea Bouguer Anomalies

Over continents, topographic masses external to the geoid are removed (Land Bouguer Effect). Over oceans, the density deficit of seawater relative to crustal rock is compensated (Seawater Bouguer Effect).

The rigorous integral for the Seawater Complete Bouguer Effect on gravity anomaly/disturbance is:

$$g_b^w = \frac{G\beta}{r}\iint_S \left[\frac{r_0}{\mathcal{L}} - \frac{r_0+d}{\sqrt{(\tilde{h}-d)^2+l^2}}\right] ds \tag{8.4}$$

where $d < 0$ is the bathymetry; $\beta = \rho - \rho_w$ is the seawater compensation density; $\tilde{h}$ is the computation point elevation relative to the sea surface; r_0 is the geocentric distance of the sea surface, ds is the area element on the sea surface; $\mathcal{L}$ is the spatial distance from ds to the computation point; and l is the straight-line distance between ds and the projection point of the computation point onto the sea surface.

Since both g^R (Eq. 8.1) and g_b^w (Eq. 8.4) are regional integrals:

- In nearshore waters, $g^R \neq 0$ due to the influence of adjacent land topography..
- In coastal lands, $g_b^w \neq 0$ due to the influence of adjacent ocean basins.

This necessitates a Land-Sea Unified Bouguer effect Algorithm. Noting that terrain elevation $h = 0$ over the ocean and bathymetry $d = 0$ over land, the integration domains for g^R and g_b^w are disjoint yet seamlessly contiguous. Summing these integrals yields the unified formulas for the Bouguer gravity anomaly and disturbance:

$$\Delta g_B = \Delta g^s - g^R - 2\pi G\rho h - g_b^w - \Delta g^c \tag{8.5}$$

$$\delta g_B = \delta g^s - g^R - 2\pi G\rho h - g_b^w - \delta g^c \tag{8.6}$$

Defining the total Classical Bouguer Effect on Gravity as:

$$g^B = g_b + g_b^w = g^R + 2\pi G\rho h + g_b^w \tag{8.7}$$

it follows that the classical Bouguer correction is unified for both gravity anomalies and gravity disturbances across land and sea.

7.8.3 Land Airy-Heiskanen Crustal Isostatic Effect

Large negative Bouguer anomalies in mountainous regions suggest compensation by mass deficits (roots) in the underlying mantle (magma layer). The Airy-Heiskanen Isostatic Model assumes:

● Floating Crust: Mountains (density ρ =2.67×10^{3}kg/m^3) float on the denser mantle (mantle density ρ_1=3.27×10^{3}kg/m^3).

● Root Formation: Topographic elevations h are compensated by mountain roots of depth b extending into the mantle.

● Hydrostatic equilibrium: The mass of the root compensates the topographic load:

$$b\Delta\rho_1 = \rho_0 h \quad \Longrightarrow \quad b = \frac{\rho_0}{\Delta\rho_1} h = 4.45h \tag{8.8}$$

where $\Delta\rho_1 = \rho_1 - \rho$ = 0.6×10^{3}kg/m^3.

The Crustal Isostatic Effect (g_I) is the gravitational attraction of this compensating root mass (which fills the density deficit). It generally opposes the sign of the Bouguer effect. With the z-axis vertical and origin 0 at sea level the effect is expressed as:

$$g_I = -G\Delta\rho_1 \iint_\sigma \int_D^{D+b} \frac{z-z'}{L^3} dz\, d\sigma \tag{8.9}$$

Note: The negative sign indicates the direction relative to the removal logic; physically, the root adds mass, increasing gravity compared to the Bouguer-reduced field.

7.8.4 Calculation of Marine and Unified Land-Sea Isostatic Gravity Anomalies

The oceanic column consists of a low-density seawater layer (ρ_w =1.03×10^{3}kg/m^3) and an oceanic crust layer with density ρ. The combined weight of these layers is insufficient to balance the buoyancy force from the underlying mantle (magma), necessitating an upward displacement of mantle material into the oceanic region, forming an anti-root.

Compensation for the seawater density deficit ($\beta = \rho - \rho_w$ =1.64×10^{3}kg/m^3) generates the Seawater Bouguer Effect, as defined in Eq. (8.4). Let d denote the bathymetry (depth). After accounting for seawater compensation, the hydrostatic equilibrium condition for the oceanic anti-root depth b' is:

$$b'\Delta\rho_1 = \beta d \quad \Longrightarrow \quad b' = \frac{\beta}{\Delta\rho_1} d = 2.73d \tag{8.10}$$

Just as the land mountain root requires mass compensation, the oceanic anti-root represents a mass excess that must be removed to achieve isostatic equilibrium. Consequently, the Oceanic Crustal Isostatic Effect (g_I^o) generally opposes the sign of the Seawater Bouguer Effect. It is expressed as:

$$g_I^o = -G\Delta\rho_1 \iint_\sigma \int_{D-b'}^{D} \frac{z-z'}{L^3} dz\, d\sigma \tag{8.11}$$

Note: The integration limits reflect the anti-root extending upwards from the compensation depth D towards the seabed.

Since both the Land Isostatic Effect (Eq. 8.9) and the Oceanic Isostatic Effect (Eq. 8.11) are regional integrals:

● In nearshore waters, the land isostatic effect is non-zero (influence of distant land roots).

● In coastal land areas, the oceanic isostatic effect is non-zero (influence of distant oceanic anti-roots).

This necessitates a Unified Land-Sea Crustal Isostatic Algorithm. Following the same logic as the unified Bouguer algorithm:

● Over the ocean ($h = 0$), there is no land root; thus, the land isostatic integral

contributes zero over oceanic cells.

● Over land ($d = 0$), there is no oceanic anti-root; thus, the oceanic isostatic integral contributes zero over land cells.

The integration domains are disjoint yet seamlessly contiguous. Summing the two integrals yields the unified formulas for the Isostatic Gravity Anomaly (Δg_I) and Isostatic Gravity Disturbance (δg_I):

$$\Delta g_I = \Delta g^s - g^B - g_I - g_I^o - \Delta g^c \tag{8.12}$$

$$\delta g_I = \delta g^s - g^B - g_I - g_I^o - \delta g^c \tag{8.13}$$

Defining the total Classical Unified Land-Sea Isostatic Effect as:

$$g^I = g_I + g_I^o \tag{8.14}$$

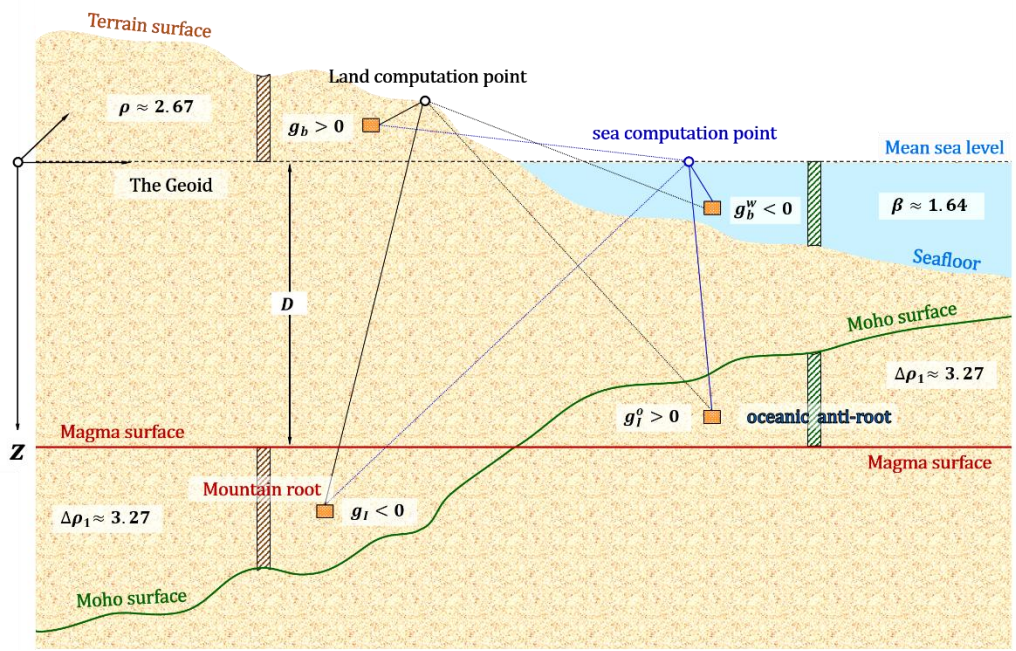

Figure 7.6: Calculation Principle for Unified Land-Sea Bouguer and Isostatic Effects on Surface Gravity

7.8.5 Physical Interpretation of Sign Conventions for Bouguer and Isostatic Effects

The sign conventions for these effects are derived from their physical mechanisms:

(a) Land Bouguer Effect ($g_b > 0$): Involves removing the excess topographic mass external to the geoid. Since topography attracts gravity positively, removing it requires a negative correction to the observed gravity. Conversely, the "effect" value g_b (the magnitude of the terrain attraction) is positive. In the reduction formula $\Delta g_B = \Delta g - g^B$, a positive g^B reduces the anomaly.

(b) Seawater Bouguer Effect ($g_b^w < 0$): Involves compensating the seawater density deficit (replacing water with rock). This adds mass, increasing gravity. However, relative to the land convention, or considering the deficit nature, the effect is defined with an opposite sign in the unified framework.

(c) Land Isostatic Effect ($g_I < 0$): Involves filling the root deficit with compensating mass.

This adds mass (increasing gravity), opposing the removal logic of the Bouguer effect. Thus, its sign is opposite to that of the Bouguer effect.

(d) Oceanic Isostatic Effect ($g_I^o > 0$): Involves removing the excess mass of the anti-root. This reduces mass (decreasing gravity), opposing the addition logic of the seawater Bouguer effect g_b^w.

● **Summary of Signs (as illustrated in Figure 7.6):**

Land Bouguer Effect: Positive (+); Seawater Bouguer Effect: Negative (−); Land Isostatic Effect: Negative (−); and Oceanic Isostatic Effect: Positive (+).

● **Magnitude Relationships:**

Principles of isostasy dictate that the compensation is partial or local.

○ On land: $|g_b| > |g_I|$. The effects partially cancel, making the Isostatic Anomaly smaller than the Bouguer Anomaly.

○ At sea: $|g_b^w| > |g_I^o|$. Similarly, the effects partially cancel.

Consequently, Isostatic Anomalies are generally smoother and smaller in magnitude than Bouguer Anomalies in most regions.

Equivalence of Topographic Effects on Gravity Field elements

● Invariance Principle: Given the invariance of the normal gravity field, various terrain effects on gravity disturbance and on gravity anomaly are strictly equal to the effects on gravity itself.

● Implementation Note: Software modules computing Local Terrain Effects, Helmert Condensation, Unified Bouguer Effects, Unified Isostatic Effects, or Residual Terrain Effects need not distinguish between anomalies and disturbances; the computed topographic correction value is the same for both.

Critical Mathematical Distinction:

While various terrain effects on δg and Δg are equal, their relationship does not satisfy the fundamental equation of physical geodesy (which relates vertical derivatives). The relationship between the terrain effects on gravity anomalies and those on height anomalies are governed by the Hotine Formula, not the Stokes Formula.

7.9 Integral Algorithm Formulas for the Anomalous Earth Gravity Field

While the global gravity field is typically modeled in the spectral domain, spatial integral algorithms are essential for local gravity field approximation. To perform integration over a finite radius in local regions, the Remove-Restore Method, based on a reference global geopotential model, is standard practice:

(1) Remove: Compute and subtract the model values of the anomalous field elements on the boundary surface to obtain residual field elements.

(2) Integrate: Apply a spatial integral algorithm with a finite radius to these residuals to derive the target residual field element at the computation point.

(3) Restore: Add the model value of the target element at the computation point to obtain the final local approximation.

7.9.1 Generalized Stokes and Hotine Integral Formulas

Given the gravity anomaly Δg on the geoid or an external equipotential surface S the disturbing potential T or height anomaly ζ at an external point $T(\theta, \lambda, r)$ is computed via the Generalized Stokes Integral:

$$T(\theta, \lambda, r) = \gamma\zeta(\theta, \lambda, r) = \frac{1}{4\pi}\iint_S \Delta g' S(r, \psi, r')ds \tag{9.1}$$

where r' is the geocentric distance of the moving element ds, and $S(r, \psi, r')$ is the Generalized Stokes Kernel:

$$S(r, \psi, r') = \frac{2}{L} + \frac{1}{r} - \frac{3L}{r^2} - \frac{5r'cos\psi}{r^2} - \frac{3r'}{r^2}cos\psi ln\frac{r - r'cos\psi + L}{2r} \tag{9.2}$$

where L being the Euclidean distance between the computation and moving points.

Singularity Handling: When the computation point coincides with the moving point, the integral becomes singular. The analytical value for this singular term is:

$$\zeta|_0 = \frac{A_0}{\gamma}\Delta g_0 \tag{9.3}$$

where A_0, Δg_0, and γ are the area, gravity anomaly, and normal gravity at the computation point, respectively.

Similarly, given the gravity disturbance δg on S, the Generalized Hotine Integral is used:

$$T(\theta, \lambda, r) = \gamma\zeta(\theta, \lambda, r) = \frac{1}{4\pi}\iint_S \delta g' H(r, \psi, r')ds \tag{9.4}$$

where the Generalized Hotine Kernel $H(r, \psi, r')$ is:

$$H(r, \psi, r') = \frac{2}{L} - \frac{1}{r'}ln\frac{r - r'cos\psi + L}{r(1 - cos\psi)} \tag{9.5}$$

The corresponding singular value is:

$$\zeta|_0 = \frac{A_0}{\gamma}\delta g_0 \tag{9.6}$$

FFT Implementation: By approximating the geocentric distances r and r' as constant mean values, these integrals transform into convolution forms, enabling rapid computation via the Fast Fourier Transform (FFT) algorithm.

Note: The Stokes boundary value problem strictly requires the boundary surface S to be an equipotential surface (e.g., the geoid which can be constructed from a global geopotential model up to degree ~360). For equipotential surfaces within an altitude of 10 km, a normal (or orthometric) equiheight surface may serve as a valid approximation.

7.9.2 Generalized Vening-Meinesz Integral Formulas

Taking horizontal derivatives of the generalized Stokes formula (9.1) in a local horizontal coordinate system yields the Generalized Vening-Meinesz Formulas for vertical deflections (ξ, η):

$$\xi = -\frac{1}{4\pi r\gamma}\iint_S \Delta g' \frac{\partial S(r, \psi, r')}{\partial \psi}\frac{\partial \psi}{\partial \varphi}ds, \quad \eta = -\frac{1}{4\pi r cos\varphi\gamma}\iint_S \Delta g' \frac{\partial S(r, \psi, r')}{\partial \psi}\frac{\partial \psi}{\partial \lambda}ds \tag{9.7}$$

From the relation:

$$cos\psi = sin\varphi sin\varphi' + cos\varphi cos\varphi' cos(\lambda' - \lambda) \tag{9.8}$$

taking horizontal derivatives on both sides gives:

$$-sin\psi\frac{\partial \psi}{\partial \varphi} = cos\varphi sin\varphi' - sin\varphi cos\varphi' cos(\lambda' - \lambda) \tag{9.9}$$

$$-sin\psi\frac{\partial\psi}{\partial\lambda}=cos\varphi cos\varphi' sin(\lambda'-\lambda) \tag{9.10}$$

Using spherical trigonometric formulas:

$$sin\psi cos\alpha=cos\varphi sin\varphi'-sin\varphi cos\varphi' cos(\lambda'-\lambda) \tag{9.11}$$

$$sin\psi sin\alpha=cos\varphi' sin(\lambda'-\lambda) \tag{9.12}$$

Combining Equations (9.9) through (9.12), we have:

$$\frac{\partial\psi}{\partial\varphi}=-cos\alpha,\quad \frac{\partial\psi}{\partial\lambda}=-cos\varphi sin\alpha \tag{9.13}$$

Substituting into Equation (9.7) yields:

$$\xi=\frac{1}{4\pi r\gamma}\iint_S \Delta g'\frac{\partial S(r,\psi,r')}{\partial\psi}cos\alpha ds,\quad \eta=\frac{1}{4\pi r\gamma}\iint_S \Delta g'\frac{\partial S(r,\psi,r')}{\partial\psi}sin\alpha ds \tag{9.14}$$

Considering $=\sqrt{r^2+r'^2-2rr'cos\psi}$, we have:

$$\frac{\partial}{\partial\psi}L=\frac{rr'}{L}sin\psi,\quad \frac{\partial}{\partial\psi}\left(\frac{1}{L}\right)=-\frac{1}{L^2}\frac{\partial}{\partial\psi}L=-\frac{rr'}{L^3}sin\psi \tag{9.15}$$

$$\frac{\partial}{\partial\psi}ln\frac{r-r'cos\psi+L}{2r}=\frac{1}{r-r'cos\psi+L}\left(\frac{rr'}{L}sin\psi+r'sin\psi\right)=\frac{r'sin\psi}{r+L-r'cos\psi}\frac{L+r}{L} \tag{9.16}$$

$$\begin{aligned}\frac{\partial}{\partial\psi}S(r,\psi,r')&=\frac{\partial}{\partial\psi}\left(\frac{2}{L}+\frac{1}{r}-\frac{3L}{r^2}-\frac{5r'cos\psi}{r^2}-\frac{3r'cos\psi}{r^2}ln\frac{r-r'cos\psi+L}{2r}\right)\\&=\frac{\partial}{\partial\psi}\frac{2}{L}-\frac{3}{r^2}\frac{\partial}{\partial\psi}L+\frac{5r'sin\psi}{r^2}+\frac{3r'sin\psi}{r^2}ln\frac{r+L-r'cos\psi}{2r}-\frac{3r'cos\psi}{r^2}\frac{\partial}{\partial\psi}ln\frac{r+L-r'cos\psi}{2r}\\&=\left(-\frac{2rr'}{L^3}-\frac{3r'}{rL}+\frac{5r'}{r^2}+\frac{3r'}{r^2}ln\frac{r-r'cos\psi+L}{2r}-\frac{3r'cos\psi}{r^2}\frac{r'}{r-r'cos\psi+L}\frac{L+r}{L}\right)sin\psi\\&=\left[-\frac{2r}{L^3}-\frac{3}{rL}+\frac{5}{r^2}+\frac{3}{r^2}ln\frac{r-r'cos\psi+L}{2r}-\frac{3r'(L+r)cos\psi}{r^2L(r-r'cos\psi+L)}\right]r'sin\psi\end{aligned} \tag{9.17}$$

Similarly, deriving from the Hotine formula (9.4) using gravity disturbances δg:

$$\xi=\frac{1}{4\pi r\gamma}\iint_S \delta g'\frac{\partial H(r,\psi,r')}{\partial\psi}cos\alpha ds,\quad \eta=\frac{1}{4\pi r\gamma}\iint_S \delta g'\frac{\partial H(r,\psi,r')}{\partial\psi}sin\alpha ds \tag{9.18}$$

Since: $\frac{\partial}{\partial\psi}ln\frac{r-r'cos\psi+L}{r(1-cos\psi)}=\frac{r(1-cos\psi)}{r-r'cos\psi+L}\frac{\left(\frac{rr'}{L}sin\psi+r'sin\psi\right)r(1-cos\psi)+(r-r'cos\psi+L)rsin\psi}{r^2(1-cos\psi)^2}$

$$=\frac{sin\psi}{r-r'cos\psi+L}\frac{\frac{L+r}{L}r'(1-cos\psi)+(r-r'cos\psi+L)}{1-cos\psi}=\left[\frac{r'(L+r)}{(r-r'cos\psi+L)L}+\frac{1}{1-cos\psi}\right]sin\psi \tag{9.19}$$

Therefore: $\frac{\partial}{\partial\psi}H(r,\psi,r')=\frac{\partial}{\partial\psi}\left(\frac{2}{L}-\frac{1}{r'}ln\frac{r-r'cos\psi+L}{r(1-cos\psi)}\right)=\frac{\partial}{\partial\psi}\frac{2}{L}-\frac{1}{r'}\frac{\partial}{\partial\psi}ln\frac{r-r'cos\psi+L}{r(1-cos\psi)}$

$$=\left[-\frac{2rr'}{L^3}-\frac{L-r}{(r-r'cos\psi+L)L}+\frac{1}{r'(1-cos\psi)}\right]sin\psi \tag{9.20}$$

These formulas allow the computation of vertical deflections at any point on the Earth's surface or in external space from gravity anomalies or disturbances defined on an equi-potential surface. Like the Stokes/Hotine integrals, they can be accelerated using FFT under the constant-radius approximation.

7.9.3 Poisson Integral Algorithm and Applications

The Poisson Integral solves the First Boundary Value Problem (Dirichlet Problem), performing analytical continuation of an anomalous field element μ (e.g., δg or ζ) from a source surface S to a target surface D at a different attitude:

$$\mu(\theta,\lambda,r)=\frac{1}{4\pi r}\int_S (\theta',\lambda',r')\frac{r^2-r'^2}{L^3}ds \tag{9.21}$$

Singularity neutralization:

When $r \to r'$ (computation point on the source surface), the kernel becomes undefined (0/0) and singular ($L \to 0$). To resolve this, we apply an identity transformation (Hofmann, 2006) to obtain the Modified Poisson Integral:

$$\mu(\theta,\lambda,r) = \frac{r'^2}{r^2}\mu(\theta,\lambda,r') + \frac{1}{4\pi r}\int_s [\mu(\theta',\lambda',r') - \mu(\theta',\lambda',r)]\frac{r^2-r'^2}{L^3}ds \tag{9.22}$$

Here, the difference term $[\mu - \mu'] \to 0$ as $L \to 0$, effectively neutralizing the singularity of the kernel and ensuring numerical stability.

Application to Gravity Gradients:

The radial disturbing gravity gradient T_{rr} can be derived by taking the radial derivative of the Poisson integral for gravity disturbance δg.

Applying the Poisson integral to the gravity disturbance δg yields:

$$\delta g(\theta,\lambda,r) = \frac{1}{4\pi r}\iint_s \delta g' \frac{r^2-r'^2}{L^3}ds \tag{9.23}$$

Considering $T_{rr} = \frac{\partial}{\partial r}\left(\frac{\partial}{\partial r}T\right) = -\frac{\partial}{\partial r}(\delta g)$, taking the radial partial derivative of both sides of Equation (9.23) gives:

$$\begin{aligned} T_{rr} &= -\frac{1}{4\pi r}\iint_s \delta g' \frac{\partial}{\partial r}\frac{r^2-r'^2}{L^3}ds \\ &= \frac{1}{4\pi r}\iint_s \delta g' \frac{r^3-5rr'^2+(r^2+3r'^2)r'^2 cos\psi}{L^5}ds \end{aligned} \tag{9.24}$$

Similar modification techniques (subtracting the computation point value inside the integral) should be applied to Eq. (9.24) to suppress singularities when computing gradients on or near the source surface.

7.9.4 Forward and Inverse Integral Operations for the Anomalous Gravity Field

(1) Computing Gravity Disturbance from Height Anomaly

Differentiating the Poisson integral for the disturbing potential T along the vertical direction yields the gravity disturbance δg :

$$\delta g = \frac{\partial T}{\partial n} \approx -\frac{\gamma \partial \zeta}{\partial r} = -\frac{\gamma}{2\pi}\iint_s \frac{\zeta-\zeta_p}{l^3}ds \tag{9.25}$$

where ∂n denotes differentiation along the vertical direction, and l is the straight-line distance between the computation point and the moving element on the equipotential boundary.

Singularity: When the computation point coincides with the moving point, the singular value is:

$$\delta g|_0 = \frac{\gamma\sqrt{A_0/\pi}}{4}\left(\zeta_{xx} + \zeta_{yy}\right) \tag{9.26}$$

where ζ_{xx}, ζ_{yy} are the second-order horizontal derivatives of the height anomaly.

Eq. (9.25) is known as the Inverse Hotine Integral. It computes gravity disturbance on an equipotential surface from height anomalies defined on the same surface.

Note: The boundary must be an equipotential surface.

(2) Computing Gravity Anomaly from Height Anomaly

Substituting the fundamental equation of physical geodesy into Eq. (9.25) yields the Inverse Stokes Integral:

$$\Delta g = -\frac{\gamma}{2\pi}\iint_s \frac{\zeta-\zeta_p}{l^3}ds - \frac{\zeta\gamma}{2r} \tag{9.27}$$

This formula derives gravity anomaly from height anomaly on an equipotential surface.

(3) Computing Height Anomaly from Vertical Deflection

$$\zeta = \frac{r}{4\pi}\iint_{\sigma} ctg\frac{\psi}{2}(\xi cos\alpha + \eta sin\alpha)\, d\sigma \tag{9.28}$$

Singularity:

$$\zeta|_0 = \frac{A_0}{4\pi}(\xi_y + \eta_x) \tag{9.29}$$

where ξ_y, η_x are are the cross-derivatives of the vertical deflection components.

(4) Computing Gravity Anomaly from Vertical Deflection

$$\Delta g = -\frac{\gamma}{4\pi}\iint_{\sigma} \left(3csc\psi - csc\psi csc\frac{\psi}{2} - tg\frac{\psi}{2}\right)(\xi cos\alpha + \eta sin\alpha)\, d\sigma \tag{9.30}$$

Singularity:

$$\Delta g|_0 = -\frac{\gamma\sqrt{A_0/\pi}}{4}(\xi_y + \eta_x) \tag{9.31}$$

(5) Computing Gravity Disturbance from Vertical deflection Integral

Combining the fundamental differential equation with Eqs. (9.28) and (9.30) yields:

$$\delta g = -\frac{\gamma}{4\pi}$$
$$\iint_{\sigma} \left(3csc\psi - csc\psi csc\frac{\psi}{2} - tg\frac{\psi}{2} - 2ctg\frac{\psi}{2}\right)(\xi cos\alpha + \eta sin\alpha)\, d\sigma \tag{9.32}$$

Singularity:

$$\delta g|_0 = -\frac{\gamma}{2\pi}\left(\sqrt{\pi A_0} + \frac{A_0}{r}\right)(\xi_y + \eta_x) \tag{9.33}$$

Eqs. (9.28), (9.30), and (9.32) constitute the Inverse Vening-Meinesz Integrals. Under the constant-radius approximation ($r \approx$const), all inverse formulas (9.25 – 9.32) can be efficiently computed using the FFT algorithm.

(6) Forward and Inverse Computation of Disturbing Gravity Gradients

Forward (Gradient to Disturbance): Compute δg at an external point from T_{rr} on an equipotential surface using the Generalized Hotine Integral:

$$\delta g(\theta, \lambda, r) = \frac{1}{4\pi}\iint_{s} T_{rr}H(r, \psi, r')ds \tag{9.34}$$

Inverse (Disturbance to Gradient): Compute T_{rr} on the surface from δg via the radial gradient integral:

$$T_{rr} = \frac{1}{2\pi}\iint \frac{\delta g - \delta g'}{l^3} ds \tag{9.35}$$

Optimization Strategy:

Optimal combination of these algorithms with "1-to-2-step residual cumulative approximation" scheme can enhance the accuracy and stability of boundary value problem solutions and short-wavelength field approximations.

7.9.5 Analytical Properties of Gravity Field Integral Kernel Functions

The kernel functions depend on the straight-line distance l, expressible via the spherical angular distance ψ. Two major challenges arise in numerical integration:

- Spectral Leakage: Due to convergence issues in the kernel functions.
- Singularity: When the computation point lies on the boundary surface ($\psi \to 0$), leading to resolution-dependent jumps in numerical results.

(1) Analysis under Spherical Approximation ($r' = r = R$):

Let $l = 2Rsin(\psi/2)$. The kernel functions on the boundary sphere are:

● Stokes Kernel:

$$S(\psi) = R \cdot S(R,\psi,R) = sin^{-1}\frac{\psi}{2} + 1 - 6sin\frac{\psi}{2} - 5cos\psi - 3cos\psi ln\frac{1-cos\psi+2sin(\psi/2)}{2}$$
$$= 1 + sin^{-1}\frac{\psi}{2} - 6sin\frac{\psi}{2} - 5cos\psi - 3cos\psi ln\left(sin\frac{\psi}{2} + sin^2\frac{\psi}{2}\right) \quad (9.36)$$

● Hotine kernel:

$$H(\psi) = R \cdot H(R,\psi,R) = 2 - ln\left(1 + sin^{-1}\frac{\psi}{2}\right) \quad (9.37)$$

● Vening-Meinesz Kernel (Derivative of Hotine):

$$V(\psi) = \frac{\partial}{\partial\psi}H(\psi) = \frac{1}{2}\frac{ctg\frac{\psi}{2}}{1+sin\frac{\psi}{2}} \quad (9.38)$$

As shown in Figure 7.7, all three kernels diverge to infinity as $\psi \to 0$ $(S, H, V \to \infty)$, necessitating singularity handling.

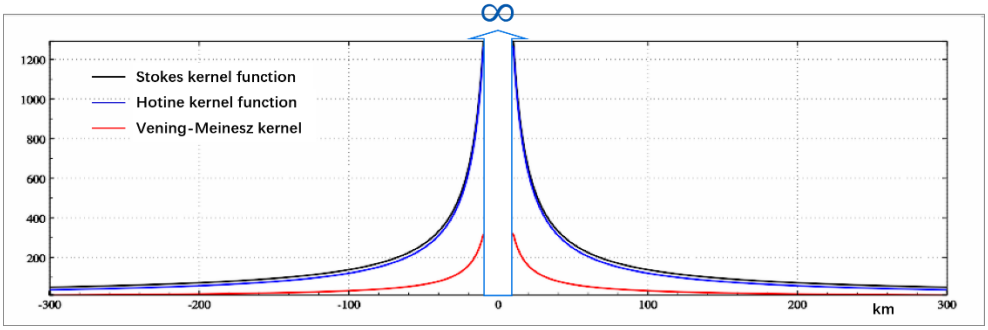

Figure 7.7: Curves of Major Gravity Field Integral Spherical Kernel Functions

(2) The Poisson Kernel Instability:

For the Poisson integral (Eq. 9.21) used for same-type continuation:

● If $r = r'$, the kernel $P(\psi) = (r^2 - r'^2)/L^3$ becomes identically zero/undefined.

● If points coincide ($L \to 0$), it becomes singular (0/0 form).

Consequently, direct Poisson integration on the same surface is numerically unstable. Effective analytical continuation requires restricting the integration range and employing modified forms (e.g., Eq. 9.22) to neutralize singularities.

(3) Recommendation on Kernel Modification:

While the Poisson integral theoretically underpins Stokes, Hotine, and Vening-Meinesz solutions, its severe high-order oscillations and non-convergence on the boundary introduce uncontrollable uncertainties. Historically, two approaches were used to mitigate this:

● Assuming isotropic random statistical properties for residual fields.

● Kernel Modification: Altering kernel functions based on spectral approximations.

However, these modification techniques rely on assumptions (statistical or data-driven) that lack a rigorous foundation in analytical gravity field theory, compromising their universality. Consequently, PAGravf4.5 does not recommend the use of gravity field integral kernel modification algorithms.

Despite numerical challenges, spatial integral formulas remain indispensable for explicitly expressing the analytical relationships between gravity field elements, serving as

the cornerstone of physical geodesy and gravity field approximation theory.

7.10 Spherical Radial Basis Function Algorithms for Gravity Field Approximation

Classical spatial gravity field boundary value theory relies on a single type of observation gravity field element on a single boundary surface. In contrast, spectral domain gravity field approximation theory does not involve boundary surfaces or boundary value conditions. It can directly approximate the all-element gravity field using multi-source heterogeneous observations via the Least Squares Method, making it the mainstream approach in modern physical geodesy. This section introduces the theory and methodology of Spherical Radial Basis Function (SRBF) spectral domain approximation.

7.10.1 Representation of the External Disturbing Potential Using SRBFs

The disturbing potential $T(\boldsymbol{x})$ at an external point $\boldsymbol{x}$ can be expressed as a linear combination of fully normalized surface spherical harmonics:

$$T(\boldsymbol{x}) = \frac{GM}{r}\sum_{n=1}^{N}\left(\frac{a}{r}\right)^n \sum_{m=-n}^{n}\bar{F}_{nm}\bar{Y}_{nm}(\boldsymbol{e}) \tag{10.1}$$

where $\boldsymbol{x} = \boldsymbol{r}\cdot\boldsymbol{e} = r(sin\theta cos\lambda, sin\theta sin\lambda, cos\theta)$ represents geocentric spherical coordinates (θ, λ, r); $\bar{F}_{nm}$ are the fully normalized Stokes coefficients (geopotential coefficients); and a is the Earth's semi-major axis. The the normalized surface spherical harmonic basis functions $\bar{Y}_{nm}(\boldsymbol{e})$ are defined on the sphere of radius a:

$$\begin{aligned} \bar{Y}_{nm}(\boldsymbol{e}) &= \bar{P}_{nm}(cos\theta)cosm\lambda, \quad \bar{F}_{nm} = \delta\bar{C}_{nm}, \quad m \geq 0 \\ \bar{Y}_{nm}(\boldsymbol{e}) &= \bar{P}_{n|m|}(cos\theta)sin|m|\lambda, \quad \bar{F}_{nm} = \bar{S}_{n|m|}, \quad m < 0 \end{aligned} \tag{10.2}$$

where $\bar{P}_{nm}(cos\theta)$ is the fully normalized associated Legendre function; n is the degree and m is the order of the geopotential coefficients.

Equivalently, these basis functions $\bar{Y}_{nm}(\boldsymbol{e})$ can be defined on a Bjerhammar sphere of radius $\mathcal{R}$. Thus, $T(\boldsymbol{x})$ can also be written as:

$$T(\boldsymbol{x}) = \frac{GM}{r}\sum_{n=1}^{N}\left(\frac{\mathcal{R}}{r}\right)^n \sum_{m=-n}^{n}\bar{E}_{nm}\bar{Y}_{nm}(\boldsymbol{e}) \tag{10.3}$$

Here, $\mathcal{R} \in (a-\delta, a+\delta)$ with $\delta \ll a$. The relationship between coefficients is $a^n\bar{F}_{nm} = \mathcal{R}^n\bar{E}_{nm}$, and the surface spherical harmonics basis functions $\{\bar{Y}_{nm}(\boldsymbol{e})\}$ in Equations (10.3) and (10.1) is identical.

Alternatively, $T(\boldsymbol{x})$ can be represented as a linear combination of K Spherical Radial Basis Functions (SRBFs):

$$T(\boldsymbol{x}) = \frac{GM}{r}\sum_{k=1}^{K} d_k\Phi_k(\boldsymbol{x}, \boldsymbol{x}_k) = \frac{GM}{r}\sum_{k=1}^{K} d_k\Phi_k(\boldsymbol{x}, \psi_k) \tag{10.4}$$

where:

$\boldsymbol{x}_k = \mathcal{R}\cdot\boldsymbol{e}_k$: The SRBF node (center) on the Bjerhammar sphere.

ψ_k: The spherical angular distance between $\boldsymbol{x}_k$ and $\boldsymbol{x}$ (the argument of the SRBF).

d_k: The SRBF coefficient.

K: The number of nodes, i.e., the number of SRBF coefficients, determining the spatial resolution.

$\Phi_k(\boldsymbol{x}, \boldsymbol{x}_k) = \Phi_k(\boldsymbol{x}, \psi_k)$: The radial basis function for the disturbing potential, which can be abbreviated as $\Phi_k(\boldsymbol{x}) = \Phi_k(\boldsymbol{x}, \boldsymbol{x}_k)$.

The SRBF can be expanded into a Legendre series:

$$\Phi_k(\boldsymbol{x},\boldsymbol{x}_k)=\Phi_k(\boldsymbol{x},\psi_k)=\sum_{n=1}^{N}\phi_n P_n(\psi_k)=\sum_{n=1}^{N}\frac{2n+1}{4\pi}B_n\left(\frac{\mathcal{R}}{r}\right)^n P_n(\psi_k) \tag{10.5}$$

where ϕ_n is the n-th degree Legendre coefficient (or shape factor), characterizing the spectral properties of the SRBF, and $\mu=\mathcal{R}/r$ is the bandwidth parameter.

Note that N (maximum degree) and K (number of nodes) are independent parameters. The N in Equation (10.5) is the maximum degree of the Legendre functions. Although it is the maximum degree in the surface spherical harmonic expansion of the disturbing potential (Equation 10.3), there is no explicit functional relationship with K, the number of SRBF coefficients representing spatial resolution.

Substituting Eq. (10.5) into (10.4) and applying the Spherical Harmonic Addition Theorem:

$$P_n(\psi_k)=P_n(\boldsymbol{e},\boldsymbol{e}_k)=\frac{4\pi}{2n+1}\sum_{m=-n}^{n}\bar{Y}_{nm}(\boldsymbol{e})\bar{Y}_{nm}(\boldsymbol{e}_k) \tag{10.6}$$

$$\begin{aligned}T(\boldsymbol{x})&=\frac{GM}{4\pi r}\sum_{n=1}^{N}(2n+1)B_n\left(\frac{\mathcal{R}}{r}\right)^n\sum_{k=1}^{K}d_k P_n(\psi_k)\\&=\frac{GM}{4\pi r}\sum_{k=1}^{K}d_k\sum_{n=1}^{N}(2n+1)B_n\left(\frac{\mathcal{R}}{r}\right)^n P_n(\psi_k)\end{aligned} \tag{10.7}$$

$$T(\boldsymbol{x})=\frac{GM}{r}\sum_{n=1}^{N}B_n\left(\frac{\mathcal{R}}{r}\right)^n\sum_{m=-n}^{n}\sum_{k=1}^{K}d_k\bar{Y}_{nm}(\boldsymbol{e})\bar{Y}_{nm}(\boldsymbol{e}_k) \tag{10.8}$$

yields the relationship between geopotential coefficients and SRBF coefficients:

$$\bar{F}_{nm}=\left(\frac{\mathcal{R}}{a}\right)^n\bar{E}_{nm}=B_n\left(\frac{\mathcal{R}}{a}\right)^n\sum_{k=1}^{K}d_k\bar{Y}_{nm}(\boldsymbol{e}_k) \tag{10.9}$$

This relation holds for global domain ($\psi_k\in[0,\pi)$). For local gravity field approximation, ψ_k acts analogously to the integration radius in spatial methods. The distribution and number K of SRBF centers determine the spatial degrees of freedom.

7.10.2 Suitable Spherical Radial Basis Functions for Gravity Field Approximation

SRBFs must satisfy Laplace's equation ($\Delta\Phi=0$). Common harmonic kernels include the Point-Mass kernel, Poisson kernel, Radial Multipole kernel, and Poisson Wavelet kernel.

(1) Analytical Forms and Normalized Representation

Let $\boldsymbol{x}$ be the computation point and $\boldsymbol{x}_k$ the SRBF node on the Bjerhammar sphere $\Omega_{\mathcal{R}}$.

● Point-Mass Kernel: An inverse multiquadric (Newtonian) kernel.

$$\Phi_{IMQ}(\boldsymbol{x},\boldsymbol{x}_k)=\frac{1}{L}=\frac{1}{|\boldsymbol{x}-\boldsymbol{x}_k|} \tag{10.10}$$

where: L is the spatial distance from $\boldsymbol{x}_k$ to $\boldsymbol{x}$. The point-mass function is also known as the Newtonian kernel function. Since $\Delta(1/L)=0$, the point-mass kernel function $\Phi_{IMQ}(\boldsymbol{x},\boldsymbol{x}_{\mathrm{k}})$ satisfies Laplace's equation.

● Poisson Kernel: Derived from the Poisson integral.

$$\Phi_P(\boldsymbol{x},\boldsymbol{x}_k)=-2r\frac{\partial}{\partial r}\left(\frac{1}{L}\right)-\frac{1}{L}=\frac{r^2-r_k^2}{L^3} \tag{10.11}$$

● Radial Multipole Kernel (Order m):

$$\Phi_{RM}^{m}(\boldsymbol{x},\boldsymbol{x}_k)=\frac{1}{m!}\left(\frac{\partial}{\partial r_k}\right)^m\frac{1}{L} \tag{10.12}$$

Note: $m=0$ yields the point-mass kernel: $\Phi_{IMQ}(\boldsymbol{x},\boldsymbol{x}_k)=\Phi_{RM}^{0}(\boldsymbol{x},\boldsymbol{x}_k)$.

● Poisson Wavelet Kernel (Order m):

$$\Phi_{PW}^{m}(\boldsymbol{x},\boldsymbol{x}_k) = 2(\chi_{m+1} - \chi_m), \quad \chi_m = \left(r_k \frac{\partial}{\partial r_k}\right)^m \frac{1}{L} \tag{10.13}$$

Note: $m = 0$ yields the Poisson kernel: $\Phi_P(\boldsymbol{x},\boldsymbol{x}_k) = \Phi_{PW}^{0}(\boldsymbol{x},\boldsymbol{x}_k)$.

(2) Computation of Spherical Radial Basis Functions

To highlight spectral properties and simplify multi-type data processing, SRBFs can be computed via their normalized Legendre series. A normalization coefficient Φ^0 is defined by evaluating the series at $\psi_k = 0$ ($P_n(1) = 1$):

$$\Phi^0 = \sum_{n=1}^{N} \frac{2n+1}{4\pi} B_n \mu^n \tag{10.14}$$

The Normalized SRBF is then:

$$\Phi_k(\boldsymbol{x},\boldsymbol{x}_k) = \frac{1}{\Phi^0}\sum_{n=1}^{N} \phi_n P_n(\psi_k) = \frac{1}{\Phi^0}\sum_{n=1}^{N} \frac{2n+1}{4\pi} B_n \mu^n P_n(\psi_k) \tag{10.15}$$

This normalization preserves the linear functional relationships between different gravity field elements (e.g., potential, anomaly, and disturbance).

Table 7.2: Disturbing Potential Spherical Radial Basis Functions and Their Legendre Coefficients

SRBF Type	Analytical Form Φ_k	Legendre Coeff. ϕ_n	Parameter B_n
Point mass kernel	$\frac{1}{L} = \frac{1}{\lvert x - x_k \rvert}$	μ^n	$\frac{1}{2n+1}$
Poisson kernel	$\frac{r^2 - r_k^2}{L^3}$	$(2n+1)\mu^n$	1
Radial multipole kernel (m)	$\frac{1}{m!}\left(\frac{\partial}{\partial r_k}\right)^m \frac{1}{L}$	$C_n^m \mu^{n-m}$ $(n \geq m)$	$\frac{C_n^m}{2n+1}\mu^{-m}$
Poisson wavelet kernel (m)	$2(\chi_{m+1} - \chi_m)$ $\chi_m = \left(r_k \frac{\partial}{\partial r_k}\right)^m \frac{1}{L}$	$(-nln\mu)^m (2n+1)\mu^n$	$(-nln\mu)^m$

(3) Series Representation of Various Anomalous Field elements Using SRBFs

Based on the definitions of anomalous field elements, the parameterized forms of SRBFs for other field types can be derived from the SRBF expansion of the disturbing potential (Eq. 10.6). By applying appropriate differential operators, we obtain:

- Disturbing Potential (Height Anomaly):

$$T(\boldsymbol{x}) = \gamma\zeta(\boldsymbol{x}) = \frac{GM}{4\pi r}\sum_{k=1}^{K} d_k \sum_n (2n+1) B_n \left(\frac{\mathcal{R}}{r}\right)^n P_n(\psi_k) \tag{10.16}$$

- Gravity Disturbance:

$$\delta g(\boldsymbol{x}) = -\frac{\partial T}{\partial r} = \frac{GM}{4\pi r^2}\sum_{k=1}^{K} d_k \sum_n (2n+1)(n+1) B_n \left(\frac{\mathcal{R}}{r}\right)^{n-1} P_n(\psi_k) \tag{10.17}$$

- Gravity Anomaly:

$$\Delta g(\boldsymbol{x}) = \frac{GM}{4\pi r^2}\sum_{k=1}^{K} d_k \sum_n (2n+1)(n-1) B_n \left(\frac{\mathcal{R}}{r}\right)^{n-1} P_n(\psi_k) \tag{10.18}$$

- Vertical Deflection Components (ξ: North-South, η: East-West):

$$\xi(\boldsymbol{x}) = \frac{GM}{4\pi r^2 \gamma}\sum_{k=1}^{K} d_k \cos\alpha_k \sum_n (2n+1) B_n \left(\frac{\mathcal{R}}{r}\right)^n \frac{\partial P_n(\psi_k)}{\partial \psi_k} \tag{10.19}$$

$$\eta(\boldsymbol{x}) = \frac{GM}{4\pi r^2 \gamma}\sum_{k=1}^{K} d_k \sin\alpha_k \sum_n (2n+1) B_n \left(\frac{\mathcal{R}}{r}\right)^n \frac{\partial P_n(\psi_k)}{\partial \psi_k} \tag{10.20}$$

- Radial Disturbing Gravity Gradient:

$$T_{rr}(\boldsymbol{x}) = \frac{GM}{4\pi r^3}\sum_{k=1}^{K} d_k \sum_n (2n+1)(n+1)(n+2)B_n \left(\frac{\mathcal{R}}{r}\right)^{n-1} P_n(\psi_k) \tag{10.21}$$

where $\mu = \mathcal{R}/r$ is the bandwidth parameter, and α_k is the geodetic azimuth of ψ_k.

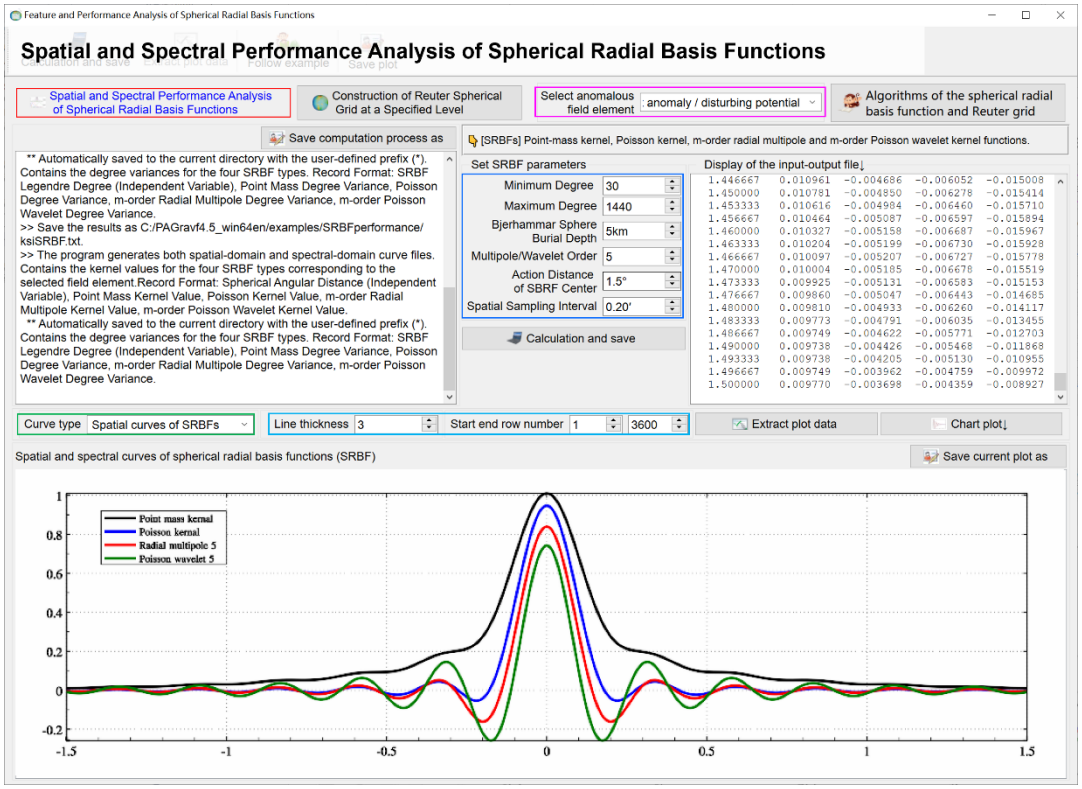

Figure 7.8: Calculation of curves of the four normalized SRBF types

Parameter Selection for Local Approximation:

In local gravity field modeling, a Remove-Restore technique is typically employed: medium-to-low frequency signals are removed using a reference global geopotential model, and residuals are approximated regionally. Consequently, the spectral bandwidth (range of degree n) and the domain of the argument ψ_k in Eqs. (10.16) – (10.21) depend critically on:

- The chosen reference global geopotential model.
- The target regional gravity field structure.
- The desired spatial resolution (controlled by the number of SRBF nodes K or the Reuter grid level Q).

These parameters should be optimized through empirical testing with actual gravity field observation data in target region.

(4) Reuter Grid Construction and Adaptive SRBF Node Design

A Spherical Equal-Area Reuter Grid provides a globally and regionally consistent framework for node distribution. Given a grid level Q, SRBF nodes (centers) are constructed such that their spatial density adapts to the distribution of observations. The level Q acts as the spatial resolution indicator, analogous to the maximum degree N_{max} of a global geopotential model.

● Unit Sphere Reuter Grid Algorithms

For an even integer level Q, the geocentric latitude interval $d\varphi$ and the latitude φ_i of the i-th row center are:

$$d\varphi = \frac{\pi}{Q}, \quad \varphi_i = -\frac{\pi}{2} + \left(i - \frac{1}{2}\right) d\varphi, \quad 1 \le i < Q \tag{10.22}$$

The number of cells J_i along the parallel at φ_i, the longitude interval $d\lambda_i$, and the approximate side length dl_i are:

$$J_i = \left[\!\left[\frac{2\pi cos\varphi_i}{d\varphi}\right]\!\right] = [\![2Qcos\varphi_i]\!], \quad d\lambda_i = \frac{2\pi}{J_i}, \quad dl_i = d\lambda_i cos\varphi_i \tag{10.23}$$

where $[\![\cdot]\!]$ denotes the floor function. Note that $dl_i \approx d\varphi$.

The relative area deviation ε_i from the equatorial cell area ds is:

$$\varepsilon_i = \frac{ds_i - ds}{ds} = \frac{dl_i - d\varphi}{d\varphi} = \frac{d\lambda_i}{d\varphi} cos\varphi_i - 1 \tag{10.24}$$

Typically, ε_i is negligible (order of 10^{-4}), ensuring near-perfect equal-area properties. For regional applications, indices i and J_i are restricted to the target latitude/longitude bounds, avoiding global grid computation.

● Adaptive SRBF Center Design

PAGravf4.5 implements an adaptive algorithm to align SRBF nodes with observation distribution density:

○ Construct a regional Reuter grid at level Q.

○ Count the number of effective observations j within each grid cell containing a potential SRBF node.

○ Pruning Rule: If j is below a user-defined minimum threshold, the corresponding SRBF node is discarded.

○ The remaining nodes form an adaptive SRBF network.

This ensures that SRBF node distribution mirrors observation distribution: regular grids yield regular nodes; irregular or clumped observations yield irregular nodes.

Global Node Count Estimate:

Setting $Q = N_{max}$, the total number of SRBF nodes K for a global grid satisfies:

$$K = \sum_{i=1}^{Q} J_i = \sum_{i=1}^{Q} [\![2Qcos\varphi_i]\!] > N_{maxn}(N_{maxn} + 2) \tag{10.25}$$

Thus, the number of SRBF coefficients slightly exceeds the number of spherical harmonic coefficients for equivalent resolution.

7.10.3 Local Gravity Field Approximation Using the Spectral Domain SRBF Method

Gravity field approximation is essentially a linear spatial transformation. Removing constant factors $(GM/(4\pi))$ and common radial terms $(1/r)$ simplifies the observation equations without altering analytical relationships. Eqs. (10.16) – (10.21) simplify to:

$$\zeta(\boldsymbol{x}) = \frac{1}{\gamma}\sum_{k=1}^{K} d_k \sum_n (2n+1) B_n \mu^n P_n(\psi_k) \tag{10.26}$$

$$\delta g(\boldsymbol{x}) = \frac{1}{r}\sum_{k=1}^{K} d_k \sum_n (2n+1)(n+1) B_n \mu^{n-1} P_n(\psi_k) \tag{10.27}$$

$$\Delta g(\boldsymbol{x}) = \frac{1}{r}\sum_{k=1}^{K} d_k \sum_n (2n+1)(n-1) B_n \mu^{n-1} P_n(\psi_k) \tag{10.28}$$

$$\xi(\boldsymbol{x}) = \frac{1}{r\gamma}\sum_{k=1}^{K} d_k \, cos\alpha_k \sum_n (2n+1) B_n \mu^n \frac{\partial P_n(\psi_k)}{\partial \psi_k} \tag{10.29}$$

$$\eta(\boldsymbol{x}) = \frac{1}{r\gamma}\sum_{k=1}^{K} d_k \, sin\alpha_k \sum_n (2n+1) B_n \mu^n \frac{\partial P_n(\psi_k)}{\partial \psi_k} \tag{10.30}$$

$$T_{rr}(\boldsymbol{x}) = \frac{1}{r^2}\sum_{k=1}^{K} d_k \sum_n (2n+1)(n+1)(n+2) B_n \mu^{n-1} P_n(\psi_k) \tag{10.31}$$

Substituting the specific B_n from Table 7.2 yields the fundamental observation equations:

$$\boldsymbol{L} = \{F(\boldsymbol{x}_i)\}^T = \boldsymbol{A}\{d_k\}^T + \boldsymbol{\varepsilon} \quad (i = 1, \cdots, M; k = 1, \cdots, K) \tag{10.32}$$

where M is the number of observations, K is the number of SRBF centers, and:

$\boldsymbol{L} = \{F(\boldsymbol{x}_1), \cdots, F(\boldsymbol{x}_M)\}^T$: Vector of observed (residual) field elements.

$\boldsymbol{d} = \{d_1, \cdots, d_K\}^T$: Vector of unknown SRBF coefficients.

$\boldsymbol{A}$: The $M \times K$ design matrix, containing the SRBF functions.

$\boldsymbol{\varepsilon}$: The $M \times 1$ observation error vector

● Technical Constraint: Uniform Action Distance

To ensure spatial consistency in the approximation quality, a critical requirement in constructing Eq. (10.32) is that all SRBF centers share an identical Action Distance (or Influence Radius) $d\,r$.

○ Definition: An observation at $\boldsymbol{x}_i$ is influenced only by SRBF nodes k satisfying $\psi_{i,k} \leq dr/\mathcal{R}$.

○ Implication: The support domain of SRBFs is truncated uniformly. This parameter $d\,r$ is conceptually equivalent to the integration radius in spatial local gravity field methods.

7.10.4 Parameter Estimation via Grouped Synergistic Adjustment of Multi-Source Heterogeneous Observations

Observations of gravity field elements exhibit distinct spatial distributions and sensitivity characteristics relative to Spherical Radial Basis Function (SRBF) coefficients. Consequently, the design matrices (sensitivity matrices) within their respective observation equations often possess disparate structural features. Formulating separate normal equations for each observation type and combining them through standard Variance Component Estimation (VCE) frequently results in unstable solutions for the SRBF coefficients due to ill-conditioning.

To address this numerical instability, a Grouped Synergistic Adjustment strategy is employed:

(a) System Grouping: Observation equations are partitioned into distinct groups based on their sensitivity patterns (design matrix $\boldsymbol{A}$) to SRBF coefficients. Observations across different groups are statistically independent, while the design matrices within a single group exhibit homogeneity. Each partition constitutes a distinct Observation System.

(b) Normalization: Normal equations for each system are formed via the Least Squares Principle and subsequently normalized to eliminate magnitude discrepancies arising from differing physical units or sensitivities.

(c) Weighted Combination: System weights are assigned based on observational quality. The normalized normal equations are weighted and summed to form a Combined Normal Equation:

$$\sum_k \left(\frac{w_k}{Q_k}\boldsymbol{A}_k^{\mathrm{T}}\boldsymbol{P}_k\boldsymbol{A}_k\right)\{d_k\}^{\mathrm{T}} = \sum_k \left(\frac{w_k}{Q_k}\boldsymbol{A}_k^{\mathrm{T}}\boldsymbol{P}_k\boldsymbol{L}_k\right) \tag{10.34}$$

where:

k =1,⋯,K : Index of the observation system; K denotes the total number of system groups..

$\boldsymbol{d} = \{d_k\}^{\mathrm{T}}$: Vector of unknown SRBF coefficients.

$\boldsymbol{A}_k, \boldsymbol{P}_k, \boldsymbol{L}_k$: Design matrix, weight matrix, and observation vector for system k, respectively.

Q_k: Normalization parameter, defined as the Root Mean Square (RMS) of the diagonal elements of $\boldsymbol{A}_k^{\mathrm{T}}\boldsymbol{P}_k\boldsymbol{A}_k$. This factor mitigates scale differences in sensitivity between disparate observation systems.

w_k: System weight, reflecting the relative quality of system k compared to others.

Key Properties:

● Independence: The internal weights P_{ki} affect only system k. Normalization via Q_k ensures that systems with sparse observations do not lose sensitivity when combined with dense systems.

● System Weight Determination: The weights w_k are estimated via a simplified Iterative VCE process:

○ Initialization: Set $w_k = 1$ and solve for preliminary SRBF coefficient vector $\boldsymbol{d}$.

○ Variance Estimation: Compute the posteriori variance σ_k^2 for each system using observation residuals.

○ Influence Propagation: Estimate the influence of σ_k^2 on the unknowns (approximated via error propagation):

$$\tilde{\sigma}_{k,s}^2 = \frac{1}{(\boldsymbol{A}_k^T\boldsymbol{A}_k)_s}\sigma_k^2, \quad w_k = \left(\sum_s \tilde{\sigma}_{k,s}^2\right)^{-1} \tag{10.35}$$

where s indexes the SRBF coefficients.

○ Iteration: Update w_k and resolve. This process typically converges within one iteration.

Note: One may analyze the variance function curves $\tilde{\sigma}_{k,s}^2$ with s as the independent variable across different systems to optimize system weights based on specific sensitivity requirements.

7.10.5 Zero-Constraint Method for SRBF Coefficients at Distant Outer Boundaries

In local gravity field approximation, Outer Boundary Constraints are necessary to suppress edge effects and stabilize the solution in regions with sparse data.

Methodology:

$$[\boldsymbol{A}^T\boldsymbol{P}\boldsymbol{A} + \epsilon\boldsymbol{\Xi}]\{d_k\}^T = \boldsymbol{A}^T\boldsymbol{P}\boldsymbol{L} \tag{10.33}$$

where:

$\boldsymbol{\Xi}$: A diagonal constraint matrix. $\Xi_{vv} = 1$ if node v is at or outside the boundary of target region; otherwise 0.

ϵ: A scaling factor, defined as the reciprocal of the RMS of the diagonal elements of $\boldsymbol{A}^T\boldsymbol{P}\boldsymbol{A}$, ensuring numerical balance between data and constraints.

Advantages: The addition of boundary conditions can weaken the need for Tikhonov-type regularization, which might otherwise distort the analytical relationships between field elements. Thus, the intrinsic functional relationships derived from potential theory are

preserved.

7.10.6 Cumulative SRBF Approximation Scheme for Residual Gravity Field elements

From a signal processing perspective, the target field element is effectively the convolution of the observed field element and the SRBF filter kernel. When the target and observed elements differ in type (e.g., approximating gravity anomalies from gravity gradients), a single SRBF function often fails to simultaneously match the spectral center and bandwidth of both elements. This mismatch can lead to spectral leakage, degrading the fidelity of the target field reconstruction. Furthermore, SRBF approximation performance depends on multiple factors beyond the Bjerhammar sphere burial depth $\mathcal{R}$ (or bandwidth parameter $\mu = \mathcal{R}/r$), including:

- The specific SRBF kernel type (Poisson, Radial multipole kernel, etc.).
- The spectral truncation limits (n_{min}, n_{max}).
- The Reuter grid level (Q) and node distribution.
- The effective action distance.

Consequently, optimizing SRBF coefficients solely by tuning the bandwidth parameter μ is insufficient to guarantee an optimal solution.

(1) Proposed Solution: Cumulative SRBF Approximation

To address this limitation, we propose a Cumulative SRBF Approximation Scheme based on the linear additivity of gravity field functionals. Unlike traditional methods that seek a single optimal μ , this scheme employs a multi-step iterative strategy:

- Multi-Spectral Fusion: Each approximation step utilizes SRBFs with distinct spectral characteristics (different centers and bandwidths).
- Parameter Flexibility: Individual steps do not require a fixed, globally optimal Bjerhammar radius $\mathcal{R}$ or μ .
- Signal Resolution: By accumulating contributions from multiple spectral bands, the method can fully resolve the target field's signal content, mitigate spectral leakage, and achieve superior approximation accuracy.

(2) Algorithmic Interpretation

Each step in the Cumulative SRBF method functions equivalently as a Remove-Restore process:

- Remove: The residual field from the previous step serves as the input.
- Restore: The current SRBF approximation models a specific spectral band of the residuals.
- Update: The new approximation is added to the cumulative model, updating the reference field for the next iteration.

This approach ensures that complex gravity field signals, which cannot be captured by a single scale parameter, are reconstructed progressively and robustly.

(3) Quantitative Criteria for Single-Step Effectiveness

The validity of each iteration within the cumulative scheme is governed by two simple and intuitive criteria:

● Spatial Regularity & Minimization: The target field element grid should remain spatially continuous and differentiable, and the standard deviation of residual observations is as small as possible.

● Convergence Behavior: As cumulative steps proceed, the statistical mean of the residual observations must converge toward zero without exhibiting significant sign reversals (indicative of over-correction or instability).

(4) Distinctive Technical Features of the PAGravf4.5 SRBF Module

(a) Strict Analytical Consistency and Error Immunity:

The approximation scheme strictly adheres to the intrinsic analytical functional relationships between gravity field elements. The approximation performance is mathematically decoupled from random observational errors, guaranteeing the internal consistency of the physical-mathematical model.

(b) Direct Full-Space, All-Element Modeling Without Traditional Pre-processing:

Capable of directly utilizing multi-source heterogeneous observations to construct all-element gravity field models on or outside the geoid. No traditional gravity reduction, upward/downward continuation, or gridding interpolation is required, thereby eliminating signal attenuation and non-analytical distortions at the source.

(c) Robust Fusion of Sparse observations:

Exhibits superior capability in leveraging and fusing sparse high-precision observation data (e.g., limited astronomical vertical deflections or GNSS-leveling sites).

(d) Advanced Quality Control and Performance Assessment:

Equipped with high-precision mechanisms for detecting observational gross errors, quantitatively assessing external accuracy metrics, and comprehensively monitoring and optimizing computational performance.

7.11 Height Systems and Height Datum: Theory and Concepts

The fundamental essence of geodetic elevation is the geopotential difference. In geodesy, elevation serves as the geometric approximation of the geopotential number in Earth's gravity field space, defined in an Earth-fixed coordinate reference system. By selecting the geoid potential W_G as the constant reference datum, the geopotential number of a terrain point represents its potential energy relative to the geoid. This constitutes a physically meaningful "physical elevation", an objective quantity inherent to the gravity field. The corresponding height system is termed the Geopotential Number System.

7.11.1 Rigorous Geodetic Definitions of Height Systems

The definition of geometric geodetic elevation must satisfy three fundamental conditions:

● Uniqueness: The elevation of any point must be single-valued.

● Measurability: Reduction corrections should be minimal to avoid significant deviations from observed leveling elevations, in local, low-order levelings.

● Equipotential Consistency: Points on an equipotential surface should possess almost identical elevations.

Geodetic elevation (orthometric or normal height) is the geometric realization of the

geopotential number within the Earth-fixed reference system, adhering to the constraints of uniqueness and measurability. The height difference between two points represents the geometric realization of their geopotential difference. The two primary forms are Orthometric Height and Normal Height, both referred to collectively as "geometric elevations."

Let W_A be the geopotential of terrain point A. Let point Q share the same ellipsoidal coordinates (latitude, longitude) as A, with its normal potential U_Q equal to W_A. By gravity field theory, the segment QA represents the height anomaly ζ_A at point A (see Figure 7.9).

All elements in Figure 7.9 reside within a unified Earth-fixed reference system with a consistent geometric scale. Arrows indicate the direction of measurement. This establishes the Earth-fixed reference system theory as the indispensable foundation for modern height systems.

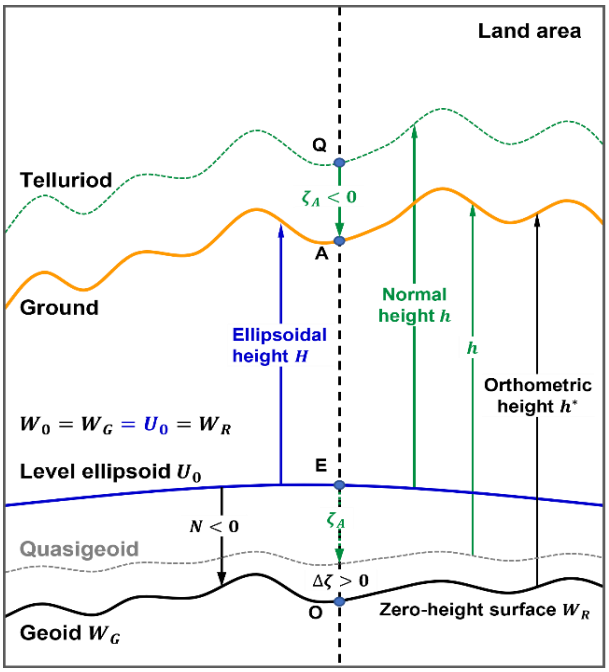

Figure 7.9： Geometric Relationships among Ellipsoidal Height, Orthometric/Normal Height, and Geoidal Height in an Earth-Fixed Reference System

(1) Physical-Geodetic Definition of the Orthometric Height System

Orthometric height h^* is defined as the ratio of the geopotential number c_A of point A to the mean gravity $\bar{g}_A$ between A and the geoid G:

$$h_A^* = \frac{W_G - W_A}{\bar{g}_A} = \frac{c_A}{\bar{g}_A} \tag{11.1}$$

The mean gravity $\bar{g}_A$ is physically defined as:

$$\bar{g}_A = \frac{1}{h_A^*}\int_0^{h^*} g(h)dh \tag{11.2}$$

where dh is the line element between the terrain surface and the geoid. Assuming a constant crustal density ρ, the mean gravity $\bar{g}_A$ can be approximated using the Prey reduction formula:

$$\bar{g}_A = g_A - \left(\frac{1}{2}\frac{\partial\gamma}{\partial h} + 2\pi G\rho\right)h_A^* \tag{11.3}$$

where g_A is the observed gravity at A, G is the gravitational constant, and $\partial\gamma/\partial h$ is the

normal gravity gradient. The resulting elevation is known as the Helmert Orthometric Height.

(2) Physical-Geodetic Definition of the Normal Height System

Normal height h is defined as the ratio of the normal geopotential number of point Q ($U_0 - U_Q$) to the mean normal gravity $\bar{\gamma}_Q$ between Q and the normal ellipsoid E:

$$h_A = \frac{U_0 - U_Q}{\bar{\gamma}_Q} \tag{11.4}$$

According to the Molodensky condition, the normal geopotential number at Q equals the actual geopotential number at A ($U_0 - U_A = c_A = W_G - W_A$). Substituting this yields the Molodensky Normal Height:

$$h_A = \frac{U_0 - U_Q}{\bar{\gamma}_Q} = \frac{W_G - W_A}{\bar{\gamma}_Q} = \frac{C_A}{\bar{\gamma}_Q} \tag{11.5}$$

where $\bar{\gamma}_Q$ is the Molodensky mean normal gravity. Given $W_G = U_0$, it follows that

$$U_Q = W_A \tag{11.6}$$

Equation (11.6) confirms that point Q lies on the equipotential surface passing through A (Fig. 7.9). China's national height system is based on this definition.

Note: The Molodensky condition here is distinct from the Molodensky Boundary Value Problem; it is the geometric realization of Bruns' formula at point A.

Since $\bar{\gamma}_Q$ ($\bar{g}_A$) is constant, normal (orthometric) height is also unique, path-independent, and measurable.

7.11.2 Concept of the Analytical Geoid and Analytical Orthometric Height

The so-called "true" geoid (or terrain-corrected geoid), which attempts to account for the topographic mass effects through reduction, suffers from decimeter-level uncertainties in continental mountainous regions. These uncertainties stem from necessary approximations in terrain density models and assumptions regarding methods of terrain mass reduction (e.g., Helmert condensation or complete Bouguer reduction). At the centimeter-level precision demanded, such a geoid fails to meet the fundamental constraints of uniqueness and precise measurability required for valid geodetic elements. Consequently, the geoidal height derived following such terrain adjustments is metrologically undefined; it is neither uniquely determinable nor does it possess an accepted concept of accuracy.

To resolve this fundamental theoretical and practical impasse, PAGravf4.5 introduces the Analytical Geoid, a well-defined geodetic element achieved via specific, theoretically consistent terrain mass reduction that preserves the potential field's invariance. Crucially, before and after this mass reduction, the geopotential (or the disturbing potential T) remains invariant everywhere across the entire ground surface and throughout the external space (or any closed surface outside the geoid). This geoidal height is defined as the Analytical Geoidal Height, which is mathematically equivalent to the analytical continuation of the height anomaly (ζ) from the ground surface (or exterior) down to the geoid.

In metrological sense, helmert orthometric height fails to qualify as a general geodetic element satisfying the uniqueness and measurability requirement. Furthermore, it does not meet the datum conditions necessary for GNSS Replacing Leveling, since rendering the relationship ($H = h^* + N$) between ellipsoidal height (H), orthometric height (h^*), and geoidal

height (N) ambiguous.

PAGravf4.5 addresses this long-standing deficiency by introducing the Analytical Orthometric Height. In this formulation, the gravity at any point along the theoretical path from the ground to the geoid is not approximated by a constant or a simplified density model. Instead, it is defined as the gravity value obtained via the analytical continuation of the external gravity field to that specific point (i.e., the analytical gravity). The mean gravity along this path is then rigorously defined as the geometric mean of these continuously varying analytical gravity values. The orthometric height derived from this rigorously defined mean gravity constitutes the Analytical Orthometric Height.

Unlike the Helmert orthometric height, both the Analytical Orthometric Height and the Normal Height strictly satisfy the datum conditions for GNSS Replacing Leveling. And the fundamental equation $H = h$ (normal height) + ζ holds with analytical rigor. Furthermore, these two height systems share a rigorous analytical functional relationship within the framework of gravity field theory. This robust and consistent theoretical foundation is not Earth-specific, two height systems can be directly extended and applied to other celestial bodies, such as the Moon and terrestrial planets.

The Analytical Orthometric Height requires no assumptions regarding crustal density. Its mean gravity can be continuously refined and updated using the latest gravity field data and models, making it a dynamic and improvable geodetic element. From the perspective of the uniqueness and measurability of geodetic elements, the Analytical Orthometric Height is more suitable for modern height datum purposes than other types of orthometric heights.

Simple calculations using global geopotential models demonstrate that, numerically, the values of the Analytical Orthometric Height and the Normal Height are globally much closer to each other than either is to the Helmert orthometric height. The discrepancy between the Analytical Orthometric Height and the Helmert orthometric height can reach approximately 60 cm at an elevation of 3,000 meters.

7.11.3 Analytical Functional Relationship between Orthometric and Normal Heights

Geodetic elevation (orthometric or normal height) is the geometric expression of geopotential in the Earth-fixed reference system. Both orthometric and normal heights are objectively unique and precisely measurable.

The ellipsoidal height H relates to orthometric height h^* and geoidal height (geoid undulation) N, as well as normal height h and height anomaly ζ, via:

$$H = h^* + N = h + \zeta \tag{11.7}$$

Equation (11.7) provides the theoretical basis for determining h^* (or h) using GNSS-derived H and a geoid model (N or ζ). The difference between orthometric and normal heights is:

$$h^* - h = \zeta - N = \Delta\zeta \tag{11.8}$$

That is, the discrepancy between the orthometricl height h^* and normal height h equals the difference between the height anomaly ζ and geoidal height N.

The integral solution to the Stokes Boundary Value Problem determines the disturbing potential everywhere outside the geoid, yielding both ζ and N (Generalized Stokes Formula).

Crucially, this solution constrains the analytical relationship between ζ and N (Zhang Chuanyin, 2017):

$$\zeta = N + \Delta\zeta = N + \int_0^{h^*} \frac{\partial \zeta}{\partial h} dh = N - \int_0^{h^*} \frac{\delta g}{\gamma} dh \tag{11.9}$$

where δg is the gravity disturbance and γ are is the normal gravity along the line element dh.

7.11.4 Applicability of the Geoid as the Zero-Elevation Surface

While orthometric and normal heights are unique and measurable geometric quantities, their physical representation (the geopotential number) involves approximations. This is an inherent characteristic of their geodetic definitions.

(1) Geodetic Basis for the Uniqueness of the Height Datum

If the normal height of point A is zero ($h_A = 0$), Substituting equation (11.5), we can obtain:

$$h_A = \frac{U_0 - U_Q}{\bar{\gamma}_Q} = \frac{W_\mathrm{G} - W_A}{\bar{\gamma}_Q} = \frac{c_A}{\bar{\gamma}_Q} = 0 \quad \Longrightarrow \quad c_A = 0, \quad W_A = W_\mathrm{G} \tag{11.10}$$

This indicates that a point with zero normal height has zero geopotential number, thus the point should lie on the geoid ($W_A = W_\mathrm{G}$).

Substituting $c_A = 0$ into the orthometric height definition (11.1) yields:

$$h_A^* = \frac{W_G - W_A}{\bar{g}_A} = \frac{c_A}{\bar{g}_A} = \frac{0}{\bar{g}_A} = 0 \tag{11.11}$$

Equation (11.11) shows that the orthometric height of point A also equals zero, $h_A^* = 0$. Consequently, a point with zero normal height also has zero orthometric height.

Conclusion: The zero-orthometric-height surface, zero-normal-height surface, zero-geopotential-number surface, and the Geoid are coincident. They all share the constant geopotential W_G. Therefore, regardless of the specific height system (Orthometric Height, Normal Height, or Geopotential Number), the geodetic height starting datum surface is only the (global or regional) Geoid.

(2) Analysis of Geoidal Geopotential Properties and Datum Nature

The geodetic definitions of orthometric and normal heights [Eqs. (11.1) and (11.5)] constitute the sole theoretical foundation in geodesy for elucidating the nature of the height starting datum and geodetic elevation. All formulas for leveling elevation difference corrections are derived from these definitions.

The definition of height system can be uniformly expressed as:

$$\mathcal{H} = \frac{W_G - W}{\mathcal{g}} = \frac{c}{\mathcal{g}} \tag{11.12}$$

where:

- If $\mathcal{g}$ represents the mean gravity between the terrain point and the geoid, Eq. (11.12) defines the Orthometric Height System.
- If $\mathcal{g}$ represents the Molodensky mean normal gravity, it defines the Molodensky Normal Height System.
- If $\mathcal{g} = 1$, it defines the Geopotential Number System.

A unique and time-invariant reference datum is a mandatory constraint for the entire geodetic discipline. Examining Eq. (11.12), since $\mathcal{g} \neq 0$, the geopotential W of a terrain point is the sole independent variable determining its orthometric (or normal) height, whereas the

geoidal geopotential W_G is a pre-defined constant. Consequently, Eq. (11.12) dictates that only the constant W_G can serve as the unique, invariant starting datum value for orthometric and normal height systems.

(3) Definition of Geoidal Geometric Deformation

The elevation of any terrain point is an objective quantity uniquely defined by its geopotential number. For a deforming Earth, the geopotential W changes objectively with time due to the redistribution of internal mass, inducing temporal variations in the geopotential number (and thus geometric elevation) at any point. Earth's deformation directly causes discrepancies in the spatial distribution of geopotential between two time epochs. This means that in the Earth-fixed reference system, the geometric positions of the geoid (W_G remains unchanged) at two epochs differ, and this difference represents the geoid's geometric deformation.

7.11.5 Issues with the Quasi-Geoid as a Datum Surface

In traditional physical geodesy, the closed surface where the ellipsoidal height equals the ground height anomaly is termed the quasi-geoid. Historically, this surface was regarded as the datum for normal heights. However, this perception contradicts the rigorous definition of normal height [Eq. (11.5)] for two reasons:

(a) Physical Inconsistency: The geopotential number on the zero-normal-height surface is zero; thus, the zero-normal-height surface is the geoid, not the quasi-geoid.

(b) Violation of Uniqueness: For two points with identical latitude and longitude but different attitudes, their height anomalies (ζ) differ. If normal heights were referenced to the quasi-geoid, there would exist two non-coincident starting points in the vertical direction for the same location, violating the uniqueness requirement of the normal height system.

Actual observation points rarely lie precisely on the specific Digital Elevation Model (DEM) surface employed to construct the ground height anomaly model. For centimeter-level applications, a height-dependent correction $\delta\zeta$, accounting for the height anomaly gradient (or gravity disturbance), should be applied:

$$\zeta = \zeta_0 + \delta\zeta = \zeta_0 + \int_{h_0}^{h} \frac{\partial \zeta}{\partial h} dh = \zeta_0 - \int_{h_0}^{h} \frac{\delta g}{\gamma} dh = \zeta_0 - \left[\frac{\delta g}{\gamma}\right](h - h_0) \tag{11.13}$$

where:

ζ: Height anomaly at the actual observation point (elevation h).

ζ_0: Height anomaly interpolated from the ground height anomaly model to the point's horizontal location.

h_0: Terrain elevation interpolated from the DTM.

$\delta g, \gamma$: Gravity disturbance and normal gravity, respectively, along the vertical segment.

$[\cdot]$: Averaging operator.

Practical Implication: For instance, using a 1′×1′ ground height anomaly model to represent the quasi-geoid can result in correction terms $\delta\zeta$ reaching decimeter-level magnitudes in regions like western China. Thus, while the normal height system is theoretically rigorous, looking the quasi-geoid as its datum surface fails to meet geodetic requirements at decimeter-level accuracy and contradicts Eq. (11.5).

Consequently, PAGravf4.5 comprehensively deemphasizes the concept of the quasi-geoid and related legacy knowledge.

7.11.6 Geometric Properties of Height Systems and Conceptual Updates

Both orthometric and normal height systems are strictly defined within the Earth-fixed reference system based on gravity field theory.

(1) Geometric Parallelism of Orthometric Heights:

Consider two surfaces of constant orthometric height, h_1' and h_2', such that their difference $\Delta h_{12}' = h_2' - h_1' = C \neq 0$ is constant. From Eq. (11.7), the ellipsoidal height difference ΔH_{12} between the two surfaces is:

$$\Delta H_{12} = H_2 - H_1 = (h_2' + N) - (h_1' + N) = h_2' - h_1' = \Delta h_{12}' = C \tag{11.14}$$

Eq. (11.14) demonstrates that the ellipsoidal height difference between two constant orthometric height surfaces equals their orthometric height difference, independent of the geoidal height N. This implies that orthometric equiheight surfaces are parallel within the Earth-fixed reference system.

● **Revised Definition:** Orthometric height is rigorously the distance from a terrain point to the geoid measured along a straight line perpendicular to the geoid. A direct corollary is that the integration path in the mean gravity definition [Eq. (11.2)] should be treated as a straight line.

● **Correction of Misconception:** The conventional view that orthometric height is the irregular curvilinear distance along the plumb line is incorrect. Due to the deflection of the vertical and the curvature of the normal gravity line, the plumb line is an irregular curve whose length exceeds the straight-line distance. This traditional interpretation lacks a rigorous geodetic foundation.

● **Limitation:** Globally parallel closed surfaces do not exist in external Earth space. Parallelism holds only in infinitesimally local spaces; thus, orthometric height possesses typical local properties.

(2) Geometric Behavior of Normal Heights:

Normal height is also unique and measurable. However, since the height anomaly ζ varies with attitude (elevation), normal equiheight surfaces are not strictly parallel in the Earth-fixed reference system. The signal of the height anomaly attenuates with increasing elevation. Consequently, the geometric shape of a normal equiheight surface becomes progressively smoother relative to the geoid as elevation increases.

(3) Conclusion:

● Orthometric Height: Offers intuitive geometric measurement properties due to the parallelism of its equipheight surfaces with the geoid.

● Normal Height: aligns more closely with gravity field properties, as its equipheight surfaces smooth out with elevation increase, reflecting the attenuation of gravitational signals.

● Both height systems possess distinct advantages, limitations, and scientific applicability. Their coexistence is both necessary and scientifically justified.